EXPERIMENTAL and MOLECULAR MEDICINE, Vol. 44, No. 5, 330-339, May 2012

Platelet-rich plasma inhibits the apoptosis of highly adipogenic homogeneous preadipocytes in an *in vitro* culture system

Yoshitaka Fukaya[1], Masayuki Kuroda[2,3,6], Yasuyuki Aoyagi[2,3], Sakiyo Asada[2,3], Yoshitaka Kubota[1], Yoshitaka Okamoto[2], Toshinori Nakayama[4], Yasushi Saito[5], Kaneshige Satoh[1] and Hideaki Bujo[3]

[1]Department of Plastic and Reconstructive Surgery
Graduate School of Medicine
Chiba University
Chiba 260-0856, Japan
[2]Center for Advanced Medicine
Chiba University Hospital
Chiba 260-0856, Japan
[3]Department of Genome Research and Clinical Application
[4]Department of Immunology
Graduate School of Medicine
Chiba University
Chiba 260-0856, Japan
[5]Chiba University
Chiba 260-0856, Japan
[6]Corresponding author: Tel, 81-43-222-7171;
Fax, 81-43-226-8130; E-mail, kurodam@faculty.chiba-u.jp
http://dx.doi.org/10.3858/emm.2012.44.5.037

Accepted 7 February 2012
Available Online 8 February 2012

Abbreviation: BIM, Bcl-2-interacting mediator of cell death

Abstract

Auto-transplantation of adipose tissue is commonly used for the treatment of tissue defects in plastic surgery. The survival of the transplanted adipose tissue is not always constant, and one of reasons is the accelerated apoptosis of the implanted preadipocytes. We have recently established highly homogeneous preadipocytes, named ccdPAs. The aim of the current study was to evaluate the regulation of the potency of platelet-rich plasma (PRP) on the apoptosis of ccdPAs *in vitro*. PRP stimulated the proliferation of the preadipocytes in a dose-dependent manner, and the stimulatory activity of 2% PRP was significantly higher than that of 2% FBS or 2% platelet-poor plasma (PPP). The presence of 2% PRP significantly inhibited serum starvation- or TNF-α/cycloheximide-induced apoptosis in comparison to 2% FBS or 2% PPP. DAPK1 and Bcl-2-interacting mediator of cell death (BIM) mRNAs were reduced in the preadipocytes cultured with 2% PRP in comparison to those cultured in 2% FBS. The gene expression levels were significantly higher in cells cultured without serum in comparison to cells cultured with 2% FBS, and the levels in the cells with 2% PRP were reduced to 5-10% of those in the cells without serum. These results indicated that ccdPAs exhibit anti-apoptotic activities, in addition to increased proliferation, when cultured in 2% PRP in comparison to the same concentration of FBS, and that this was accompanied with reduced levels of DAPK1 and BIM mRNA expression in *in vitro* culture. PRP may improve the outcome of transplantation of adipose tissue by enhancing the anti-apoptotic activities of the implanted preadipocytes.

Keywords: adipocytes; apoptosis; Bcl-2-like protein 11; death-associated protein kinase; platelet-rich plasma; tissue transplantation

Introduction

Aspirated fat is a common source of autologous tissue transplantation for the correction of tissue defects in plastic and reconstructive surgery (Billings and May, 1989; Patrick, 2000, 2001). Aspirated fat contains multipotential preadipocytes and progenitor cells, which have been utilized as a source of cell-based regenerative medicine (Stashower *et al.*, 1999; Zuk *et al.*, 2001; Gimble *et al.*, 2007; Yoshimura *et al.*, 2009; Bauer-Kreisel *et al.*, 2010; Sterodimas *et al.*, 2010). Although several different techniques of fat grafting have been developed, the outcomes of the transplantation vary widely. The most important factor required for successful grafting is to optimize the survival of the transplanted preadipocytes and other cells in the graft. In previous studies, we and others have shown that various cytokines are involved in the efficient cell survival of the implants (Kimura *et al.*, 2003;

Yamaguchi *et al.*, 2005; Cho *et al.*, 2006; Torio-Padron *et al.*, 2007; Kuramochi *et al.*, 2008; Ning *et al.*, 2009).

Platelet rich plasma (PRP) (Eppley *et al.*, 2006; Foster *et al.*, 2009; Redler *et al.*, 2011) has been widely applied for practical medicine, such as aesthetic plastic surgery and the treatment of soft-tissue ulcers (Welsh, 2000; Man *et al.*, 2001; Margolis *et al.*, 2001; Bhanot and Alex, 2002; Martinez-Zapata *et al.*, 2009; Sclafani, 2009). Once activated, platelets secrete various bioactive cytokines, including platelet-derived growth factor (PDGF) and transforming growth factor beta 1 (TGF-β1), which increase angiogenesis and cell proliferation relevant to soft tissue regeneration. PRP has been applied for fat grafting, and in fact, has been shown to improve the survival of implanted adipose tissue in patients (Abuzeni and Alexander, 2001; Sadati *et al.*, 2006; Cervelli *et al.*, 2009). Thus, the use of PRP has been broadened to the tissue-engineering field using adipose tissue-derived multi-potential cells (Anitua *et al.*, 2006; Muller *et al.*, 2009). PRP is also expected to function as an autologous fibrin-based scaffold for transplanted cells (Anitua *et al.*, 2006; Wu *et al.*, 2009; Kang *et al.*, 2011). In fact, recent our study showed that fibrin-based scaffold decreased the apoptotic cell death of murine ccdPAs in mice transplantation model (Aoyagi *et al.*, 2011).

We have recently identified proliferative preadipocytes, ceiling culture-derived proliferative adipocytes (ccdPAs), as homogeneous cells suitable for *ex vivo* gene therapy applications *via* autologous transplantation (Asada *et al.*, 2011; Kuroda *et al.*, 2011). The ccdPAs are characterized by their high proliferative capacity with spontaneous adipogenic potential in scaffold fibrin gel culture (Aoyagi *et al.*, 2012). The establishment of a highly homogenous preadipocyte line made it possible to perform examinations to identify the optimal scaffolds and cytokines that can be used to improve the survival of transplanted preadipocytes. We herein studied the effects of PRP, and an autologous cytokine cocktail, on the apoptotic properties of preadipocytes using the ccdPAs.

Results

PRP inhibits fibrin scaffold gel shrinkage and improves the viability of ccdPAs in 3-dimensional culture

We have recently established a 3-dimensional (3-D) culture system for ccdPAs using fibrin gel (FG) (Aoyagi *et al.*, 2012). Using the 3-D culture system, the effects of PRP on the gel shrinkage and cell viability were analyzed in comparison to FBS. The FG/ccdPAs were formed and maintained in culture medium containing 10% FBS for 16 hr. The culture medium was replaced with fresh medium containing 2% PRP, 2% FBS or 10% FBS, or with medium without serum, and cells were subsequently incubated for an additional 24 hr.

The resulting gel sizes varied among the cultures grown in each type of medium. The gels without serum or with 2% FBS showed a drastic volume reduction, while the volumes of the gels cultured with 10% FBS or 2% PRP were not obviously reduced (Figure 1A). The culture supernatants were collected from each well and LDH activity was measured to evaluate the viability of cells. The LDH activity significantly decreased in the culture medium with 2% PRP in comparison to the medium with 2% or 10% FBS (Figure 1B). TUNEL staining of the gel sections showed the number of apoptotic cells to significantly decrease in the medium with 2% PRP in comparison to the medium with 2% FBS (1.5 ± 1.1% vs 9.8 ± 1.9%, $P < 0.05$). These results suggested that 2% PRP inhibits the shrinkage of FG/ccdPAs gels, and improves the cell viability in comparison to the same concentration of FBS.

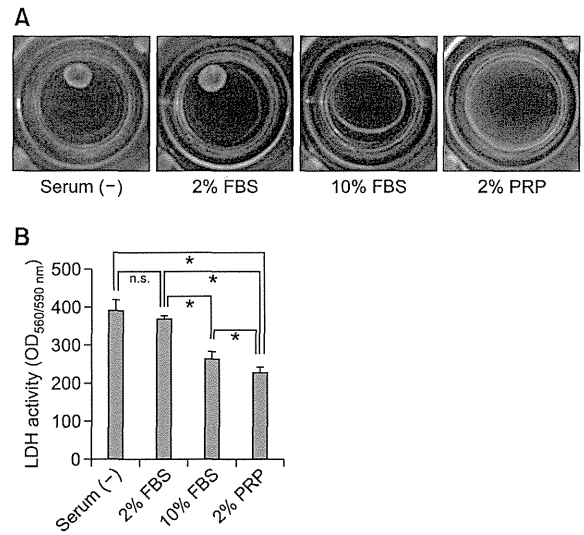

Figure 1. The effects of platelet-rich plasma (PRP) on the 3-dimensional culture of ccdPAs. 100 μl of fibrin gels containing 1×10^7 cells/ml of ccdPAs (FG/ccdPAs) were formed in cell culture insert and incubated in DMEM/HAM with 10% FBS for 16 hrs. The medium was replaced by DMEM/HAM in the presence or absence of different concentrations of FBS or PRP. (A) Photographs of FG/ccdPAs in the inserts were taken after 24 hr of culture. (B) The culture supernatant was collected from each well and the LDH activities expressed by the fluorescence of resorufin generated by coupled enzymatic reaction were examined. *$P < 0.05$.

PRP has a high proliferation-inducing potential for ccdPAs in plate culture

In order to evaluate the function of PRP on cell survival in the gel, we next examined the effects of PRP on the proliferation of ccdPAs in comparison to FBS. The cells (2.5×10^5 cells) were seeded and incubated with DMEM/HAM containing 20% FBS in 10 cm dishes for 16 hr. The media was replaced with medium containing 2% PRP, 2% FBS, or 10% FBS, and the cells were then cultured for 3 days. The cell appearance was not apparently changed among the ccdPAs cultured for 3 days in plates with media containing 2% PRP, 2% FBS, or 10% FBS (Figure 2A). To examine the cell proliferation, 2×10^3 cells of ccdPAs were seeded onto 96 well plates and incubated at 37°C for 24 hr. The media was replaced with medium with or without 2% PRP, 2% FBS, or 10% FBS (Day 0), and the cells were cultured for 3 days. The number of cells in each well was evaluated by measuring the DNA content. In contrast to the observation that the cell numbers on Day 3 were not significantly changed in comparison to those at Day 0 in the cultures incubated in medium containing 2% FBS, the cell numbers were significantly increased in cells cultured in the medium with 10% FBS or 2% PRP, and notably, the number of cells on Day 3 in the medium containing 2% PRP was significantly increased in comparison to the cells cultured with 10% FBS (Figure 1B). The cell numbers in the media with various concentrations of PRP showed a dose-dependent increase up to 5% PRP; the number of cells present in the media with 0.5-1% PRP was almost equivalent to that of the cells cultured with 5-10% FBS (Figure 2C). These results indicated that the proliferation-inducing potential of PRP for ccdPAs was higher in comparison to that of FBS.

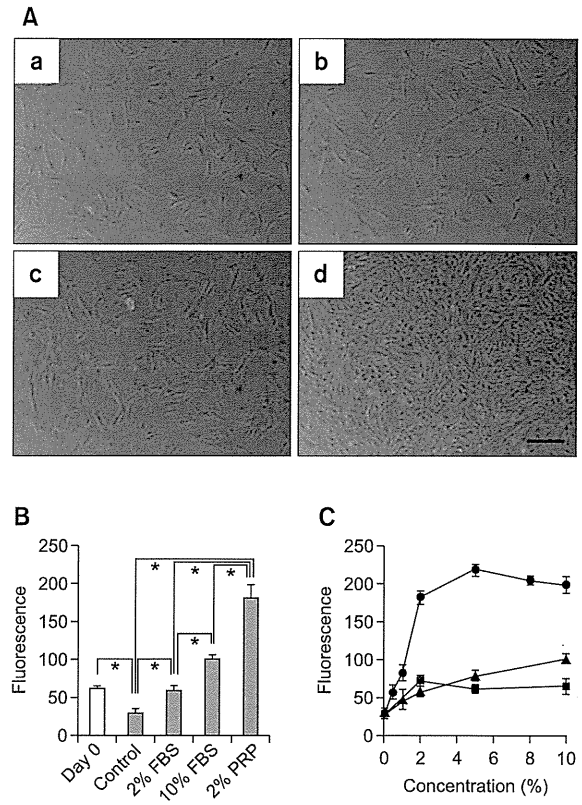

Figure 2. Platelet-rich plasma (PRP) promotes the proliferation of ccdPAs. (A) Photographs of ccdPAs were taken after 3 days in culture containing DMEM/F12-HAM in the absence of serum (a) or the presence of 2% (b) or 10% (c) FBS or 2% (d) PRP. The scale bar indicates 200 μm. (B) Cells were seeded into 96 well plates and incubated in DMEM/F12-HAM containing 20% FBS for 24 hr. The culture medium was then replaced with DMEM/F12-HAM in the absence of serum (control) or presence of 2% FBS or 10% FBS or 2% PRP. After 3 days in CO_2 incubator, the cell number in each well was examined by DNA content in comparison to those on day 0 (open bar). The values for the serum (-), 10% FBS, and 2% PRP groups were significantly different compared with those on Day 0 (*$P < 0.05$). (C) The cell numbers were examined in wells cultured in DMEM/F12-HAM containing various concentrations of PRP (circle), FBS (triangle), and PPP (square) after 3 days of culture similarly as Figure 2B. The growth stimulatory effect was not significantly different between 10% and 20% FBS and PPP (data not shown).

PRP inhibits the apoptosis of ccdPAs

The high proliferation-inducing property of PRP for ccdPAs in culture prompted us to further analyze PRP for protective effects against apoptosis in ccdPAs, since PRP is rich in cytokines and proteinases involved not only in proliferation, but also in regulating apoptosis (Eppley *et al.*, 2004, 2006; Foster *et al.*, 2009; Redler *et al.*, 2011). The protection of the cells from death may contribute to their longer survival after transplantation, together with a high potential for proliferation. To investigate the possibility, the ccdPAs (1×10^6 cells) were seeded and incubated in a 10 cm dish with DMEM/HAM medium containing 20% FBS for 16 hr, and subsequently incubated with the medium with or without 2% FBS, 2% PRP, or 2% PPP. After incubation for 8 hr, the cells were collected and stained with Annexin V-FITC. The flow cytometric analysis showed that 5.5% of cells were identified as Annexin V positive in the medium without serum (Figure 3A). The number of apoptotic cells was significantly decreased in the media with 2% FBS, 2% PRP, or 2% PPP in comparison to that in the cells cultured in serum-free medium. Among the various supplements, 2% PRP drastically reduced the number of apoptotic cells in comparison to 2% FBS or 2% PPP. ERK1/2 phosphorylation was examined to further analyze the protective effect of PRP against apoptosis, because the activation of the

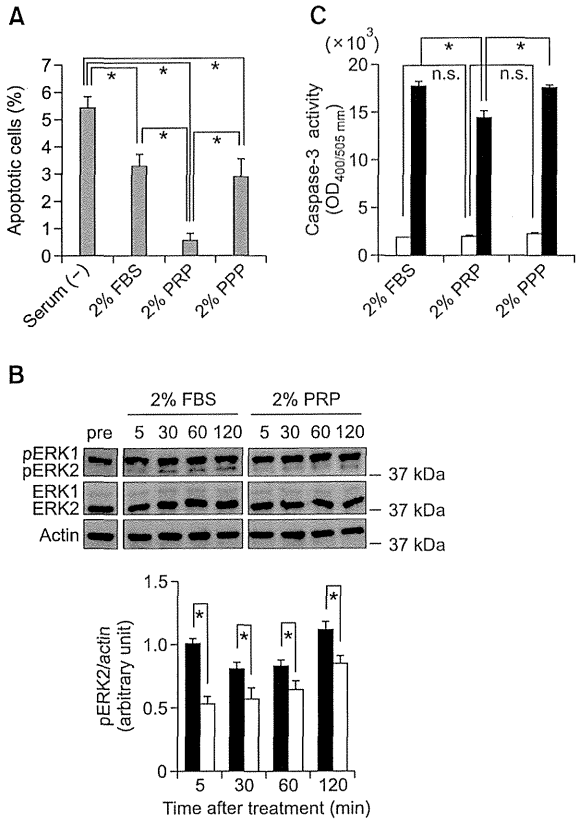

Figure 3. PRP decreased the apoptotic cell death and caspase 3 activity induced by TNF-α and cycloheximide in ccdPAs. (A) ccdPAs were seeded and incubated for 16 hr with medium containing 20% FBS, and the medium was then replaced with fresh medium without serum (Serum (-)) or with media containing 2% PRP, FBS, or PPP, and the cells were subsequently incubated at 37°C for 8 hr. The cells were then collected, stained by Annexin V-FITC and propidium iodide (PI), and analyzed using a Tali™ Image Based Cytometer (Life technologies). FITC-positive/PI-negative cells were considered to be apoptotic cells. $^*P < 0.05$. (B) After incubation for 16 hr with medium containing 20% FBS, ccdPAs were pretreated for 2 hr with the medium containing 2% PRP or FBS. The cells were treated with TNF-α and cycloheximide for 5, 30, 60, and 120 min in the medium with 2% FBS (closed bar) or 2% PRP (open bar). Cell lysates were prepared at each time point as well as pretreatment (pre) and then were subjected to an immunoblot analysis of phosphorylated or unphosphorylated form of ERK1/2, and Actin. Results of densitometric analysis of phosphorylated form of ERK2 (pERK2) is shown below. After normalization of signals of pERK2 by Actin, each value of pERK2 was expressed as the fold increase of that at 5 min with 2% FBS. $^*P < 0.05$. (C) After pretreatment for 2 hr with the medium containing 2% PRP, FBS, or PPP, the cells were incubated for 3 hr in the absence (open bars) or presence (closed bars) of TNF-α and cycloheximide, which induce apoptotic cell death. The caspase-3 activity in the lysates of collected cells were measured. $^*P < 0.05$.

cascade is important for apoptosis *via* various intracellular signals including TNF-α (Cawthorn and Sethi, 2008; Mebratu and Tesfaigzi, 2009; Cagnol and Chambard, 2010). The cells were incubated with 2% PRP, FBS, or PPP for 2 hr, and apoptosis was induced by TNF-α and cycloheximide. Phosphorylation was detected following treatment with TNF-α and cycloheximide for 5 min in the cells cultured with 2% FBS. A densitometric analysis showed the amount of phosphorylated ERK2, and not phosphorylated ERK1, to significantly decrease in the medium with 2% PRP in comparison to the medium with 2% FBS (Figure 3B). The caspase-3 activity induced by TNF-α and cycloheximide for 3 hr were also significantly decreased in ccdPAs in the medium with 2% PRP in comparison to the cells cultured with 2% FBS or 2% PPP (Figure 3C). Thus, the apoptosis of ccdPAs was inhibited by culturing them in the medium with 2% PRP *in vitro*.

PRP almost completely inhibits the expression of the pro-apoptotic genes, DAPK1 and BIM, in ccdPAs after serum starvation

In order to identify the molecules involved in the anti-apoptotic effects of PRP on ccdPAs in culture, the expression profiles of representative apoptosis-related genes were examined using a PCR array profiler. The cells (2.5×10^5 cells) were seeded into 10 cm dishes and incubated in DMEM/HAM containing 20% FBS for 16 hr. The media was replaced with DMEM/HAM containing 2% PRP or FBS, the cells were incubated for 3 days, and the total RNA was isolated from the cultured cells to analyze the expression of apoptosis-related genes. Two independent experiments showed that, among the 84 genes examined, there were 8 genes with a more than 2-fold increase in expression, and 9 genes with a more than 2-fold decrease in expression in the cells cultured in the medium with 2% PRP compared with those cultured in the medium with 2% FBS (Table 1). We focused our interest on two genes, DAPK1 (reduced to 7.4% of the expression level observed with FBS) and BCL2L11 (also called BIM, reduced to 18.9% of the level observed with FBS), as representative genes with the obvious downregulation in the medium with 2% PRP (Figure 4). DAPK1 and BIM have been shown to be one of master regulators of cell death (Gozuacik and Kimchi, 2006), and is essential for BAX-dependent cell death (Kim *et al.*, 2009; Ren *et al.*, 2010), respectively.

The role of DAPK1 and BIM genes in apoptosis of preadipocytes was investigated by examining the effect of serum starvation of cells incubated with PRP on the expressions of these genes. The ccdPAs (2.5×10^5 cells) were seeded into 10 cm dishes and incubated in DMEM/HAM containing 20% FBS for 16 hr. The medium was replaced by medium containing 10% FBS (control), 2% FBS, 2% PRP, or 2% PPP, the cells were cultured for 3 days and the expression of DAPK1 and BIM were

Table 1. Apoptosis-related genes affected by PRP

Unigene	Refseq	Symbol	Description	Fold change
Downregulated				
Hs.380277	NM_004938	DAPK1	Death-associated protein kinase 1	13.5803 ↓
Hs.469658	NM_006538	BCL2L11	BCL2-like 11 (apoptosis facilitator)	5.2596 ↓
Hs.5353	NM_001230	CASP10	Caspase 10, apoptosis-related cysteine peptidase	4.0726 ↓
Hs.591834	NM_003844	TNFRSF10A	Tumor necrosis factor receptor superfamily, member 10a	3.967 ↓
Hs.513667	NM_003946	NOL3	Nucleolar protein 3 (apoptosis repressor with CARD domain)	2.8887 ↓
Hs.501497	NM_001252	CD70	CD70 molecule	2.8129 ↓
Hs.87247	NM_003806	HRK	Harakiri, BCL2 interacting protein (contains only BH3 domain)	2.5816 ↓
Hs.710305	NM_004536	NAIP	NLR family, apoptosis inhibitory protein	2.3876 ↓
Hs.643120	NM_000875	IGF1R	Insulin-like growth factor 1 receptor	2.1732 ↓
Upregulated				
Hs.127799	NM_001165	BIRC3	Baculoviral IAP repeat-containing 3	10.851 ↑
Hs.462529	NM_003790	TNFRSF25	Tumor necrosis factor receptor superfamily, member 25	4.0981 ↑
Hs.478275	NM_003810	TNFSF10	Tumor necrosis factor (ligand) superfamily, member 10	4.0907 ↑
Hs.654459	NM_001561	TNFRSF9	Tumor necrosis factor receptor superfamily, member 9	2.9875 ↑
Hs.522506	NM_021138	TRAF2	TNF receptor-associated factor 2	2.8331 ↑
Hs.9216	NM_001227	CASP7	Caspase 7, apoptosis-related cysteine peptidase	2.2033 ↑
Hs.145726	NM_001205	BNIP1	BCL2/adenovirus E1B 19kDa interacting protein 1	2.0258 ↑
Hs.194726	NM_004874	BAG4	BCL2-associated athanogene 4	2.0241 ↑

Genes identified as having a change in expression > 2-fold induced by the addition of PRP in comparison to 2% FBS are shown.

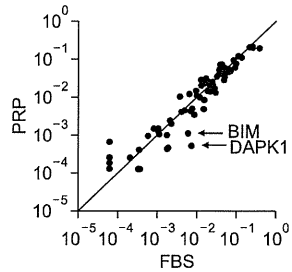

Figure 4. The results of the analysis of the expression of apoptosis-related genes affected by PRP. Total RNA was extracted from the cells cultured in the presence of 2% FBS or 2% PRP for 72 hr. The total RNA was subjected to cDNA synthesis and subsequent quantification of the mRNA expression for various apoptosis-related genes. The fold-changes in the quantified mRNA amounts compared to the average value of house-keeping genes were plotted for each gene (x-axis; cultured in 2% FBS, y-axis; cultured in 2% PRP).

analyzed. The DAPK1 mRNA level was increased 10.6-fold by serum starvation in comparison to the level in the cells cultured with 10% FBS, and the mRNA level was decreased to that of 10% FBS by the presence of 2% PRP. It is worth noting that, although the mRNA levels of DAPK1 in the cells cultured with 2% FBS and 2% PPP significantly decreased in comparison to those cultured without serum, the reductions were by 20.4% and 11.9%, respectively, which were less than that (93.6%) induced by culture in 2% PRP. The BIM mRNA levels were also drastically increased in the cells cultured in serum free medium in comparison to those cultured in the medium with 10% FBS (Figure 2C). The mRNA levels were reduced to those observed in the cells cultured with 10% FBS by the addition of 2% PRP. Again, the potential of 2% PRP to inhibit the mRNA expression of the target gene (by 87.2%) was significantly higher than that of the 2% FBS (54.1%) or 2% PPP (72.2%). Thus, PRP almost completely inhibited the expression of apoptosis-related genes induced by serum starvation.

Discussion

PRP inhibited the volume reduction of the 3D gels embedded with ccdPAs, the homogeneous preadipocytes, in comparison to the same concentration of FBS, and this was accompanied by increased cell viability in the gel. These observations prompted us to analyze the effects of PRP on the apoptosis and proliferation of the ccdPAs. The results showed that 2% PRP had a higher inhibitory effect on the apoptotic cell death of ccdPAs than 2% FBS or 2% PPP (Figure 3). A comparison between 2% PRP and 2% FBS by a gene expression profile analysis revealed that PRP downregulated 11% of the 84 representative apoptosis-related genes and upregulated 10% of the 84 representative apoptosis-related genes (Figure 4 and Table 1). The most drastically reduced genes were DAPK1, the protein product of which plays important roles in a wide range of signal transduction pathways with diverse outcomes, such as apoptosis, autoph-

agy and immune responses (Lin *et al.*, 2010), and BIM, encoding one of the BH3-only proteins, which is a critical regulator of apoptosis in many cell types (Ramesh *et al.*, 2009). The induction of these genes by apoptotic stimuli was almost completely prevented in the presence of PRP (Figure 5).

PRP, a concentrate of physiological cytokines, has been widely utilized as an injectable material in the clinic since the 1970s to enhance soft and hard tissue healing (Andia *et al.*, 2010; Lopez-Vidriero *et al.*, 2010; Redler *et al.*, 2011; Yu *et al.*, 2011), mainly by stimulating cell proliferation and angiogenesis in the injured tissues. PRP promotes the growth of various cells, including tissue-derived progenitor cells (Liu *et al.*, 2002; Lucarelli *et al.*, 2003; Doucet *et al.*, 2005; Frechette *et al.*, 2005; Vogel *et al.*, 2006; Kakudo *et al.*, 2008; Kurita *et al.*, 2008; Cervelli *et al.*, 2009; Chieregato *et al.*, 2011), and increases the revascularization of the transplanted tissues (Bir *et al.*, 2009). Based on these findings, the clinical applications of PRP have been broadened to recommend its use as an additive to tissue/cell transplantation therapies in plastic and reconstructive surgeries, and more recently in regenerative medicine. In fact, PRP has been shown to improve the fat graft survival (Abuzeni and Alexander, 2001; Sadati *et al.*, 2006; Cervelli *et al.*, 2009; Nakamura *et al.*, 2010; Pires Fraga *et al.*, 2010; Oh *et al.*, 2011) and bone and periodontal regenerations *via* cell transplantation (Tobita *et al.*, 2008; Chen *et al.*, 2010; Yamada *et al.*, 2010; Arvidson *et al.*, 2011).

In order to apply PRP for clinical transplantation therapy using preadipocytes cultured *in vitro*, it is necessary to elucidate the effects of PRP on cell survival in the grafts. However, the mechanisms by which PRP increases graft survival have not been well-characterized so far. The current study showed that PRP strongly induces the proliferation of ccdPAs, preadipocytes which were previously shown to be more adipogenic than ASCs (Asada *et al.*, 2011), compared with FBS at an equivalent concentration. Vogel *et al.* (2006) described that, because the addition of 2% PRP did not result in sufficient thrombocyte-clot formation to maintain a clot in the medium, a higher concentration of PRP, 3%, was evaluated for the stimulation of the MSC proliferation. In this study, to evaluate the efficacy of lower concentrations of PRP, the PRP was activated by thrombin to release cytokines (Aiba-Kojima *et al.*, 2007) prior to the experiments. As a result, 2% PRP showed almost the same effects on proliferation as 10% PRP, indicating its usability as a substitute for FBS in the expansion of preadipocytes for clinical applications. Finally, 2% PRP showed anti-apoptotic activities on the

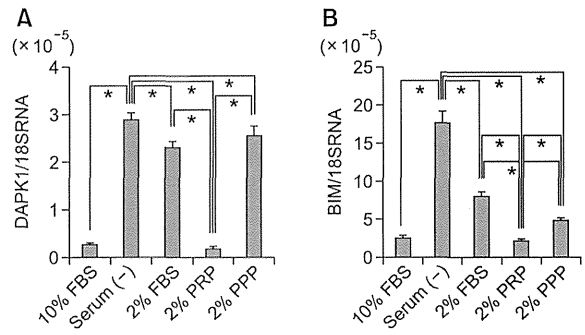

Figure 5. Serum starvation induced the expression of the DAPK1 and BIM genes, which was prevented by culture with 2% PRP. The ccdPAs were seeded and incubated for 16 hr in DMEM/HAM containing 20% FBS, and the culture medium was then replaced with medium without serum (Serum (-)), or with 2% or 10% FBS, 2% PRP, or 2% PPP, followed by incubation for an additional 72 hr. Quantitative reverse transcription-polymerase chain reaction (RT-PCR) was performed to evaluate the mRNA expression levels of DAPK1 (A) and BIM (B). The quantification of the given genes was expressed as relative mRNA level compared with a control after normalization to 18S RNA. $^*P < 0.05$.

preadipocytes, providing evidence that it can be used as an efficacious additive in the cell transplantation cocktail.

We observed that the expression of the DAPK1 and BIM genes was substantially upregulated by serum starvation in ccdPAs. However, the addition of PRP in the growth media effectively inhibited the apoptosis and downregulated the expression of these genes. TGF-β has been shown to induce the expression of DAPK1 and BIM, and to lead to subsequent apoptosis in other cell types (Jang *et al.*, 2002; Wildey *et al.*, 2003; Ramjaun *et al.*, 2007; Yu *et al.*, 2008). PRP may therefore inhibit the TGF-β-induced apoptosis cascade(s) during serum starvation in ccdPAs. Further analyses are needed to elucidate the mechanism(s) underlying the inhibitory potential of PRP on the expression levels of the representative apoptotic genes. The gene expression analysis also showed that PRP regulated the expression levels of genes involved in TNF signaling (TNFRSF10A, TNFRSF25, TNFSF10, TNFRSF9, and TRAF2), and of the Bcl protein superfamily, with its related proteins (HRK, BNIP1, and BAG4) (Table 1). The changes in the expression of these genes may also improve the survival of ccdPAs by modulating the apoptotic stimuli, considering that TNF-α signaling plays an important role in the regulation of the adipose tissue mass (Warne, 2003).

In conclusion, PRP inhibits cell apoptosis as well as or better than FBS, and also promotes the proliferation of the ccdPAs. The gene expression analyses identified that the DAPK1 and BIM genes were the most highly downregulated apoptosis-related

genes by PRP treatment in the preadipocytes. The identified characteristics of PRP with regard to the preadipocytes have advantages including increases in the cell number and improved cell survival in the transplanted grafts. Together with our findings for the efficacies of fibrin scaffold in transplantation of ccdPAs (Aoyagi *et al.*, 2011), the use of PRP for cell preparation and implantation of fat tissues and/or propagated cells may provide the graft with stable long-term survival after auto-transplantation.

Methods

Cell culture

Subcutaneous adipose tissues were obtained from healthy donors after informed consent was obtained, with approval from the ethics committee of Chiba University School of Medicine, and all studies were performed according to the guidelines of the Declaration of Helsinki. The preparation of the ceiling culture-derived proliferative adipocytes (ccdPAs) was performed as described previously (Kuroda *et al.*, 2011). Dulbecco's modified Eagle's medium/F12-HAM (DMEM/HAM, Sigma-Aldrich, St. Louis, MO) supplemented with 20% fetal bovine serum (FBS, SAFC Biosciences, Lenexa, KS) and 40 μg/ml gentamicin (GENTACIN, Schering-Plough Co., Kenilworth, NJ) was used as the culture media, unless otherwise noted in the text.

Preparation of PRP

Human PRP and PPP were prepared from healthy donors as follows; 52 ml of blood was obtained from the donors and mixed with 8 ml of Anticoagulant Citrate Dextrose Solution Formula A (ACD-A, TERUMO, Tokyo, Japan) solution, and transferred to 15 ml tubes. The tubes were centrifuged at 300 × *g* for 15 min at 20°C. The plasma and the buffy coat below the plasma were collected and transferred to new tubes. Secondary centrifugation was performed at 2000 × *g* for 15 min at 20°C. The clear supernatant (plasma) was decanted off until 6 ml was left and the middle portion of supernatant (plasma) was taken to be used as PPP. Finally, the remaining supernatant including the buffy coat was taken to be used as PRP. The platelet number of each product was automatically measured (XS 800i, sysmex Japan). The PRP utilized in this study contained 8.6 × 10^6 platelets/μl, which was approximately 7-fold concentrated from the original concentration in whole human plasma. Preparations of serum lysates containing platelet-released growth factors were essentially performed according to the method described by Aiba-Kojima *et al.* (2007). In brief, 2 U/ml of thrombin (Astellas Pharma Inc. Tokyo, Japan) was added to PRP and PPP, and the samples were agitated for 1 hr at 37°C and then incubated overnight at 4°C. Platelet bodies and any remaining fibrin were eliminated by centrifugation (2000 × *g* for 10 min), and the supernatants were obtained for the PRP and PPP. The serum samples were frozen at -20°C and thawed at 37°C before use. The growth medium was supplemented with 2 U/ml of heparin (Novo-Heparin, 5,000 units/5 ml for Injection, Mochida Pharm. Co. Tokyo, Japan).

Culture on fibrin scaffolds

Bolheal (The Chemo-Sero-Therapeutic Research Institute, Kumamoto, Japan) was used as a clinically available material to generate the fibrin gel. Fibrinogen and thrombin solutions were diluted with Ringer's Solution (Fuso Pharmaceutical Industries, Osaka, Japan) containing 0.5% human serum albumin (Mitsubishi Tanabe Pharma., Tokyo, Japan). The ccdPAs were suspended at 1 × 10^7 cells/ml by the diluted fibrinogen and thrombin solution. The final concentration of fibrinogen was 4 mg/ml and the thrombin solution was used at 1 U/ml. To form fibrin clots, 50 μl of the cell-fibrinogen suspension was added to each cell culture insert (Falcon 3104; Becton Dickinson, Franklin Lakes, NJ), then shortly thereafter, 50 μl of the cell-thrombin suspension was added into the insert, mixed by pipetting, and incubated at room temperature for 2 h. The inserts with fibrin clots were put on 12 well culture plates, and culture media were added to the inserts and wells. The plates were incubated at 37°C for 12 h in a 5% CO_2 incubator, and the media were replaced by fresh media containing FBS or PRP.

LDH assay

LDH released into the culture supernatant from the FG/ccdPA was measured using the CytoTox-One Homogeneous Membrane Integrity Assay kit (Promega, Madison, WI). A 100 μl sample of each culture supernatant was collected and added into to a 96-well plate. An equal volume of CytoTox-One Reagent was added and incubated for 10 min. Fifty μl of Stop Solution was added and the sample fluorescence was measured on a fluorescence microplate reader (SPECTRA max GEMINI XPS, Molecular Devices, Carlsbad, CA) using a wavelength of 560 nm/590 nm for excitation/emission. The original culture medium before the serum concentration was changed served as a pre-treatment control sample and the control value was subtracted from the value obtained after incubation with the medium containing different concentrations of serum.

Cell proliferation assay

The cell proliferation was examined using the CyQUANT^R Cell Proliferation Assay Kit (Life Technologies, Carlsbad, CA). Cells were seeded into 96 well plates at a density of 2 × 10^3 cells per well with DMEM/HAM/20% FBS. After 24 h, the culture medium was removed and changed to fresh DMEM/HAM without serum, or with FBS, PRP or PPP. After 3 days, the microplates were gently inverted and blotted onto paper towels to remove the medium from the wells. The microplates were then frozen and stored at -80°C and thawed at room temperature prior to analysis. CyQUANT GR dye/cell-lysis buffer was added to each well. Cells were incubated at room temperature for 5 min and the sample fluorescence was measured on a fluorescence microplate reader (SPECTRA max GEMINI XPS, Molecular Devices) using wavelength of 480 nm/520 nm for excitation/emission.

Induction of apoptosis, and the annexin V binding and caspase 3 activity assays

The cells were seeded into 10 cm dishes at a density of 1×10^6 cells per well with DMEM/HAM/20%FBS. After 24 h, the culture medium was removed and changed to fresh DMEM/HAM with 2% FBS, 2% PRP or 2%PPP. After 2 h, apoptosis was induced by the addition of 100 ng/ml TNF-α (Peprotech, Rocky Hill, NJ) and 100 μg/ml cycloheximide (CHX, Sigma-Aldrich). After 3 h, the culture supernatant was collected, and the cells were detached by TrypZean treatment. The detached cells were suspended in the collected culture supernatant. Subsequently, the cells were stained with Annexin V-FITC using a Tali™ Apoptosis kit (Life Technologies). Stained cells were analyzed by a Tali™ Image Based Cytometer (Life technologies). Cell lysates at the concentration of 1×10^4 cells/μl were prepared from the cells treated to induce apoptosis, and the caspase 3 activity levels were measured by a caspase-3/CPP32 Fluorometric Assay Kit (Biovision, Mountain View, CA). To examine the phosphorylation status of ERK1/2, the cells were scraped off at each time point in PBS and washed. The cells were pelleted and lysed by RIPA buffer (Wako Pure Chemical Industries, Ltd. Osaka, Japan), and the protein concentration was determined by Quant-iT Protein Assay Kit (Life technologies), and 5 μg of protein were analyzed by Western blotting using anti-ERK1 and anti-ERK1/2 (pT202/pY204) as primary antibodies (BD Biosciences, Franklin Lakes, NJ). Mouse TrueBlot ULTRA HRP-conjugated Anti-Mouse IgG (eBioscience, Inc. San Diego, CA) was used as a secondary antibody, and the signals were detected by SuperSignal® West Femto Maximum Sensitivity Substrate (Thermo Fisher Scientific Inc.) with LAS1000 apparatus (FUJI film, Tokyo, Japan). ERK signals were normalized using Actin signals detected by Anti-Actin monoclonal antibody (clone AC-40, Sigma-Aldrich).

Gene expression analysis

Cells (2.5×10^5 cells) were seeded into 10 cm dish with DMEM/HAM/20% FBS and cultured for 16 h. The culture medium was changed to fresh DMEM/HAM supplemented with 2% FBS or 2% PRP, and the cells were further incubated for 72 h. The total RNA from cultured cells was extracted using a RT^2 RNA Isolation Kit (SA Bioscience, Frederick, MD). Complementary DNA was generated from 1 μg of total RNA using the RT^2 First Strand Kit. An Apoptosis Reverse Transcriptase RT^2 profiler PCR array and RT^2 Real-Time SYBR Green/ROX PCR Mix (SA Bioscience, Frederick, MD) were used to identify the genes affected by PRP according to manufacturer's instruction. The data were analyzed by web-based data analysis software provided by the manufacturer. The probe and primer sets used to quantify the mRNA for the DAPK1 and BIM genes were purchased from Applied Biosystems (Life Technologies). The quantification of given genes was expressed as the relative mRNA level compared with a control after normalization to 18S RNA. All the real-time PCR were performed using an ABI 7500 real-time PCR apparatus.

Statistical analysis

The data are presented as the means ± S.D. Statistical comparisons were made by Student's *t*-test or an ANOVA followed by the post-hoc Tukey test using the *SPSS* software program. In all cases, *P*-values < 0.05 were considered to be significant.

Acknowledgements

We thank Dr. Fumiaki Matsumoto, Mr. Shunichi Konno, Dr. Shigeaki Tanaka, and Mr. Masayuki Aso for helpful and valuable suggestions about our research. This study was supported by Health and Labour Sciences Research Grants for Translational Research, Japan (H. B.), and in part by the Global COE Program (Global Center for Education and Research in Immune System Regulation and Treatment), MEXT, Japan (Y.O., Y.N., and H.B.).

References

Abuzeni PZ, Alexander RW. Enhancement of autologous fat transplantation with platelet rich plasma. Am J Cosmet Surg 2001;18:59-70

Aiba-Kojima E, Tsuno NH, Inoue K, Matsumoto D, Shigeura T, Sato T, Suga H, Kato H, Nagase T, Gonda K, Koshima I, *Takahashi K, Yoshimura K.* Characterization of wound drainage fluids as a source of soluble factors associated with wound healing: comparison with platelet-rich plasma and potential use in cell culture. Wound Repair Regen 2007; 15:511-20

Andia I, Sanchez M, Maffulli N. Tendon healing and platelet-rich plasma therapies. Expert Opin Biol Ther 2010; 10:1415-26

Anitua E, Sanchez M, Nurden AT, Nurden P, Orive G, Andia I. New insights into and novel applications for platelet-rich fibrin therapies. Trends Biotechnol 2006;24:227-34

Aoyagi Y, Kuroda M, Asada S, Bujo H, Tanaka S, Konno S, Tanio M, Ishii I, Aso M, Saito Y. Fibrin glue increases the cell survival and the transduced gene product secretion of the ceiling culture-derived adipocytes transplanted in mice. Exp Mol Med 2011;43:161-7

Aoyagi Y, Kuroda M, Asada S, Tanaka S, Konno S, Tanio M, Aso M, Okamoto Y, Nakayama T, Saito Y, Bujo H. Fibrin grue is a candidate scaffold for long-term therapeutic protein expression in spontaneously differentiated adipocytes *in vitro*. Exp Cell Res 2012;318:8-15

Arvidson K, Abdallah BM, Applegate LA, Baldini N, Cenni E, Gomez-Barrena E, Granchi D, Kassem M, Konttinen YT, Mustafa K, Pioletti DP, Sillat T, Finne-Wistrand A. Bone regeneration and stem cells. J Cell Mol Med 2011;15:718-46

Asada S, Kuroda M, Aoyagi Y, Fukaya Y, Tanaka S, Konno S, Tanio M, Aso M, Satoh K, Okamoto Y, Nakayama T, Saito Y, Bujo H. Ceiling culture-derived proliferative adipocytes retain high adipogenic potential suitable for use as a vehicle for gene transduction therapy. Am J Physiol Cell Physiol 2011;301:C181-5

Bauer-Kreisel P, Goepferich A, Blunk T. Cell-delivery therapeutics for adipose tissue regeneration. Adv Drug Deliv Rev 2010;62:798-813

Bhanot S, Alex JC. Current applications of platelet gels in facial plastic surgery. Facial Plast Surg 2002;18:27-33

Billings E Jr, May JW Jr. Historical review and present status of free fat graft autotransplantation in plastic and reconstructive surgery. Plast Reconstr Surg 1989;83:368-81

Bir SC, Esaki J, Marui A, Yamahara K, Tsubota H, Ikeda T, Sakata R. Angiogenic properties of sustained release platelet-rich plasma: characterization in-vitro and in the ischemic hind limb of the mouse. J Vasc Surg 2009;50: 870-9.e2

Cagnol S, Chambard JC. ERK and cell death: mechanisms of ERK-induced cell death-apoptosis, autophagy and senescence. FEBS J 2010;277:2-21

Cawthorn WP, Sethi JK. TNF-a and adipocyte biology. FEBS Lett 2008;582:117-31

Cervelli V, Gentile P, Scioli MG, Grimaldi M, Casciani CU, Spagnoli LG, Orlandi A. Application of platelet-rich plasma in plastic surgery: clinical and *in vitro* evaluation. Tissue Eng Part C Methods 2009;15:625-34

Chen FM, Zhang J, Zhang M, An Y, Chen F, Wu ZF. A review on endogenous regenerative technology in periodontal regenerative medicine. Biomaterials 2010;31:7892-927

Chieregato K, Castegnaro S, Madeo D, Astori G, Pegoraro M, Rodeghiero F. Epidermal growth factor, basic fibroblast growth factor and platelet-derived growth factor-bb can substitute for fetal bovine serum and compete with human platelet-rich plasma in the ex *vivo* expansion of mesenchymal stromal cells derived from adipose tissue. Cytotherapy 2011; 13:933-43

Cho SW, Kim I, Kim SH, Rhie JW, Choi CY, Kim BS. Enhancement of adipose tissue formation by implantation of adipogenic-differentiated preadipocytes. Biochem Biophys Res Commun 2006;345:588-94

Doucet C, Ernou I, Zhang Y, Llense JR, Begot L, Holy X, Lataillade JJ. Platelet lysates promote mesenchymal stem cell expansion: a safety substitute for animal serum in cell-based therapy applications. J Cell Physiol 2005;205: 228-36

Eppley BL, Woodell JE, Higgins J. Platelet quantification and growth factor analysis from platelet-rich plasma: implications for wound healing. Plast Reconstr Surg 2004;114:1502-8

Eppley BL, Pietrzak WS, Blanton M. Platelet-rich plasma: a review of biology and applications in plastic surgery. Plast Reconstr Surg 2006;118:147e-59e

Foster TE, Puskas BL, Mandelbaum BR, Gerhardt MB, Rodeo SA. Platelet-rich plasma: from basic science to clinical applications. Am J Sports Med 2009;37:2259-72

Frechette JP, Martineau I, Gagnon G. Platelet-rich plasmas: growth factor content and roles in wound healing. J Dent Res 2005;84:434-9

Gimble JM, Katz AJ, Bunnell BA. Adipose-derived stem cells for regenerative medicine. Circ Res 2007;100:1249-60

Gozuacik D, Kimchi A. DAPk protein family and cancer. Autophagy 2006;2:74-9

Jang CW, Chen CH, Chen CC, Chen JY, Su YH, Chen RH. TGF-b induces apoptosis through Smad-mediated expression of DAP-kinase. Nat Cell Biol 2002;4:51-8

Kakudo N, Minakata T, Mitsui T, Kushida S, Notodihardjo FZ, Kusumoto K. Proliferation-promoting effect of platelet-rich plasma on human adipose-derived stem cells and human dermal fibroblasts. Plast Reconstr Surg 2008;122:1352-60

Kang YH, Jeon SH, Park JY, Chung JH, Choung YH, Choung HW, Kim ES, Choung PH. Platelet-rich fibrin is a Bioscaffold and reservoir of growth factors for tissue regeneration. Tissue Eng Part A 2011;17:349-59

Kim H, Tu HC, Ren D, Takeuchi O, Jeffers JR, Zambetti GP, Hsieh JJ, Cheng EH. Stepwise activation of BAX and BAK by tBID, BIM, and PUMA initiates mitochondrial apoptosis. Mol Cell 2009;36:487-99

Kimura Y, Ozeki M, Inamoto T, Tabata Y. Adipose tissue engineering based on human preadipocytes combined with gelatin microspheres containing basic fibroblast growth factor. Biomaterials 2003;24:2513-21

Kuramochi D, Unoki H, Bujo H, Kubota Y, Jiang M, Rikihisa N, Udagawa A, Yoshimoto S, Ichinose M, Saito Y. Matrix metalloproteinase 2 improves the transplanted adipocyte survival in mice. Eur J Clin Invest 2008;38:752-9

Kurita M, Aiba-Kojima E, Shigeura T, Matsumoto D, Suga H, Inoue K, Eto H, Kato H, Aoi N, Yoshimura K. Differential effects of three preparations of human serum on expansion of various types of human cells. Plast Reconstr Surg 2008;122:438-48

Kuroda M, Aoyagi Y, Asada S, Bujo H, Tanaka S, Konno S, Tanio M, Ishii I, Machida K, Matsumoto F, Satoh K, Aso M, Saito Y. Ceiling culture-derived proliferative adipocytes are a possible delivery vehicle for enzyme replacement therapy in lecithin: cholesterol acyltransferase deficiency. Open Gene Ther J 2011;4:1-10

Liu Y, Kalen A, Risto O, Wahlstrom O. Fibroblast proliferation due to exposure to a platelet concentrate *in vitro* is pH dependent. Wound Repair Regen 2002;10:336-40

Lin Y, Hupp TR, Stevens C. Death-associated protein kinase (DAPK) and signal transduction: additional roles beyond cell death. FEBS J 2010;277:48-57

Lopez-Vidriero E, Goulding KA, Simon DA, Sanchez M, Johnson DH. The use of platelet-rich plasma in arthroscopy and sports medicine: optimizing the healing environment. Arthroscopy 2010;26:269-78

Lucarelli E, Beccheroni A, Donati D, Sangiorgi L, Cenacchi A, Del Vento AM, Meotti C, Bertoja AZ, Giardino R, Fornasari PM, Mercuri M, Picci P. Platelet-derived growth factors enhance proliferation of human stromal stem cells. Biomaterials 2003;24:3095-100

Man D, Plosker H, Winland-Brown JE. The use of autologous platelet-rich plasma (platelet gel) and autologous platelet-poor plasma (fibrin glue) in cosmetic surgery. Plast Reconstr Surg 2001;107:229-37;discussion 238-9

Margolis DJ, Kantor J, Santanna J, Strom BL, Berlin JA.

Effectiveness of platelet releasate for the treatment of diabetic neuropathic foot ulcers. Diabetes Care 2001;24:483-8

Martinez-Zapata MJ, Marti-Carvajal A, Sola I, Bolibar I, Angel Exposito J, Rodriguez L, Garcia J. Efficacy and safety of the use of autologous plasma rich in platelets for tissue regeneration: a systematic review. Transfusion 2009;49: 44-56

Mebratu Y, Tesfaigzi Y. How ERK1/2 activation controls cell proliferation and cell death: Is subcellular localization the answer? Cell Cycle 2009;8:1168-75

Muller AM, Davenport M, Verrier S, Droeser R, Alini M, Bocelli-Tyndall C, Schaefer DJ, Martin I, Scherberich A. Platelet lysate as a serum substitute for 2D static and 3D perfusion culture of stromal vascular fraction cells from human adipose tissue. Tissue Eng Part A 2009;15:869-75

Nakamura S, Ishihara M, Takikawa M, Murakami K, Kishimoto S, Yanagibayashi S, Kubo S, Yamamoto N, Kiyosawa T. Platelet-rich plasma (PRP) promotes survival of fat-grafts in rats. Ann Plast Surg 2010;65:101-6

Ning H, Liu G, Lin G, Yang R, Lue TF, Lin CS. Fibroblast growth factor 2 promotes endothelial differentiation of adipose tissue-derived stem cells. J Sex Med 2009;6:967-79

Oh DS, Cheon YW, Jeon YR, Lew DH. Activated platelet-rich plasma improves fat graft survival in nude mice: a pilot study. Dermatol Surg 2011;37:619-25

Patrick CW Jr. Adipose tissue engineering: the future of breast and soft tissue reconstruction following tumor resection. Semin Surg Oncol 2000;19:302-11

Patrick CW Jr. Tissue engineering strategies for adipose tissue repair. Anat Rec 2001;263:361-6

Pires Fraga MF, Nishio RT, Ishikawa RS, Perin LF, Helene A Jr, Malheiros CA. Increased survival of free fat grafts with platelet-rich plasma in rabbits. J Plast Reconstr Aesthet Surg 2010;63:e818-22

Ramesh S, Wildey GM, Howe PH. Transforming growth factor b (TGFb)-induced apoptosis: the rise & fall of Bim. Cell Cycle 2009;8:11-7

Ramjaun AR, Tomlinson S, Eddaoudi A, Downward J. Upregulation of two BH3-only proteins, Bmf and Bim, during TGF beta-induced apoptosis. Oncogene 2007;26:970-81

Redler LH, Thompson SA, Hsu SH, Ahmad CS, Levine WN. Platelet-rich plasma therapy: a systematic literature review and evidence for clinical use. Phys Sportsmed 2011;39:42-51

Ren D, Tu HC, Kim H, Wang GX, Bean GR, Takeuchi O, Jeffers JR, Zambetti GP, Hsieh JJ, Cheng EH. BID, BIM, and PUMA are essential for activation of the BAX- and BAK-dependent cell death program. Science 2010;330:1390-3

Sadati KS, Corrado AC, Alexander RW. Platelet-rich plasma (PRP) utilized to promote greater graft volume retention in autologous fat grafting. Am J Cosmet Surg 2006;23:203-11

Sclafani AP. Applications of platelet-rich fibrin matrix in facial plastic surgery. Facial Plast Surg 2009;25:270-6

Stashower M, Smith K, Williams J, Skelton H. Stromal progenitor cells present within liposuction and reduction abdominoplasty fat for autologous transfer to aged skin. Dermatol Surg 1999;25:945-9

Sterodimas A, de Faria J, Nicaretta B, Pitanguy I. Tissue engineering with adipose-derived stem cells (ADSCs): current and future applications. J Plast Reconstr Aesthet Surg 2010;63:1886-92

Tobita M, Uysal AC, Ogawa R, Hyakusoku H, Mizuno H. Periodontal tissue regeneration with adipose-derived stem cells. Tissue Eng Part A 2008;14:945-53

Torio-Padron N, Borges J, Momeni A, Mueller MC, Tegtmeier FT, Stark GB. Implantation of VEGF transfected pre-adipocytes improves vascularization of fibrin implants on the cylinder chorioallantoic membrane (CAM) model. Minim Invasive Ther Allied Technol 2007;16:155-62

Vogel JP, Szalay K, Geiger F, Kramer M, Richter W, Kasten P. Platelet-rich plasma improves expansion of human mesenchymal stem cells and retains differentiation capacity and *in vivo* bone formation in calcium phosphate ceramics. Platelets 2006;17:462-9

Warne JP. Tumour necrosis factor a: a key regulator of adipose tissue mass. J Endocrinol 2003;177:351-5

Welsh WJ. Autologous platelet gel: clinical function and usage in plastic surgery. Cosmet Dermatol 2000;13:13-8

Wildey GM, Patil S, Howe PH. Smad3 potentiates transforming growth factor b (TGFβ)-induced apoptosis and expression of the BH3-only protein Bim in WEHI 231 B lymphocytes. J Biol Chem 2003;278:18069-77

Wu W, Zhang J, Dong Q, Liu Y, Mao T, Chen F. Platelet-rich plasma - A promising cell carrier for micro-invasive articular cartilage repair. Med Hypotheses 2009;72:455-7

Yamada Y, Nakamura S, Ito K, Sugito T, Yoshimi R, Nagasaka T, Ueda M. A feasibility of useful cell-based therapy by bone regeneration with deciduous tooth stem cells, dental pulp stem cells, or bone-marrow-derived mesenchymal stem cells for clinical study using tissue engineering technology. Tissue Eng Part A 2010;16:1891-900

Yamaguchi M, Matsumoto F, Bujo H, Shibasaki M, Takahashi K, Yoshimoto S, Ichinose M, Saito Y. Revascularization determines volume retention and gene expression by fat grafts in mice. Exp Biol Med (Maywood) 2005;230:742-8

Yoshimura K, Suga H, Eto H. Adipose-derived stem/progenitor cells: roles in adipose tissue remodeling and potential use for soft tissue augmentation. Regen Med 2009;4:265-73

Yu J, Zhang L, Chen A, Xiang G, Wang Y, Wu J, Mitchelson K, Cheng J, Zhou Y. Identification of the gene transcription and apoptosis mediated by TGF-β-Smad2/3-Smad4 signaling. J Cell Physiol 2008;215:422-33

Yu W, Wang J, Yin J. Platelet-rich plasma: a promising product for treatment of peripheral nerve regeneration after nerve injury. Int J Neurosci 2011;121:176-80

Zuk PA, Zhu M, Mizuno H, Huang J, Futrell JW, Katz AJ, Benhaim P, Lorenz HP, Hedrick MH. Multilineage cells from human adipose tissue: implications for cell-based therapies. Tissue Eng 2001;7:211-28

Atherosclerosis 228 (2013) 193–197

Contents lists available at SciVerse ScienceDirect

Atherosclerosis

journal homepage: www.elsevier.com/locate/atherosclerosis

Amelioration of circulating lipoprotein profile and proteinuria in a patient with LCAT deficiency due to a novel mutation (Cys74Tyr) in the lid region of LCAT under a fat-restricted diet and ARB treatment

Shokichi Naito [a,*], Mariko Kamata [a], Masako Furuya [a], Miyuki Hayashi [a], Masayuki Kuroda [b,c], Hideaki Bujo [b], Kouju Kamata [a]

[a] Department of Nephrology in Internal Medicine, Kitasato University Hospital and Kitasato University School of Medicine, 1-15-1 Kitasato, Minami-ku, Sagamihara, Kanagawa 252-0375, Japan
[b] Department of Genome Research and Clinical Application, Graduate School of Medicine, Chiba University, Chiba, Japan
[c] Center for Advanced Medicine, Chiba University Hospital, Chiba University, Chiba, Japan

ARTICLE INFO

Article history:
Received 21 September 2012
Received in revised form
31 January 2013
Accepted 26 February 2013
Available online 14 March 2013

Keywords:
Familial LCAT deficiency
Novel gene mutation
Cys74Tyr
Fat-restriction diet
Circulating lipoprotein profile
Renal function

ABSTRACT

Familial lecithin-cholesterol acyltransferase (LCAT) deficiency is a hereditary disease characterized by an abnormal lipid profile, corneal opacity, anemia and progressive renal disease. We report a patient with complete loss of LCAT activity due to a novel *lcat* gene mutation of Cys74Tyr in the lid region of LCAT protein. Esterification of cholesterol in this patient was disturbed by disruption of a substrate binding loop of Cys50-Cys74 in LCAT protein. She had progressive renal dysfunction, proteinuria, corneal opacity, anemia and an abnormal lipid profile. Her serum lipids showed a significant increase in abnormal lipoproteins at the original position in agarose gel electrophoresis and VLDL-cholesterol, and a severe decrease in serum HDL-cholesterol. Lipoprotein analyzes also revealed the presence of an abnormal midband lipoprotein, and a maturation disturbance of HDL particles. Renal function and proteinuria improved following the adoption of a fat-restricted diet and administration of an angiotensin II receptor blocker. The abnormal lipoproteins also decreased after this treatment.

1. Introduction

Lecithin-cholesterol acyltransferase (LCAT) deficiency is an uncommon autosomal recessive disorder which results from a gene mutation of LCAT. Since the first identification of LCAT as a unique plasma enzyme [1], 86 mutations in the LCAT gene have been described. Patients with LCAT deficiency show an abnormal circulating lipoprotein profile as a result of the disturbed esterification of free cholesterol incorporated into high-density lipoproteins. Increased plasma concentrations of unesterified cholesterol, triglyceride (TG) and phosphatidylcholine result in lipid deposition in the tissue. LCAT deficiency develops as two clinically distinct syndromes, familial LCAT deficiency (FLD) and fish eye disease (FED). Patients with FLD show corneal opacities, hemolytic anemia, and progressive renal disease [2]. Renal disease occurs as a result of the loss of enzyme activity against β-lipoproteins rather than against α-lipoproteins. Meanwhile, FED patients develop corneal opacities as a result of a partial deficiency in LCAT activity.

A number of approaches to the treatment of LCAT deficiency have been proposed. LCAT replacement therapy by plasma transfusion produced a marked improvement in the deranged composition of TG-rich lipoproteins and Apo-E concentrations [3,4]. Recent advances in gene therapy have allowed the transplantation of *ex vivo* lcat gene-transduced adipocytes and subsequent production of human LCAT protein in circulating plasma [5,6]. Further, a clinical trial of synthetic LCAT in patients with coronary arterial disease is also currently underway at NIH (NCT01554800). In contrast, a fat-restriction diet improves the hypertriglyceridemia in these patients by reducing TG-rich lipoproteins. The lipid-lowering drugs nicotinic acid and fenofibrate have been shown to ameliorate renal function and proteinuria [7], and corticosteroids and renin–angiotensin–aldosteron (RAA) system blockers such as ACE inhibitors and angiotensin II receptor blockers (ARB) also decreased proteinuria [8–10].

Here, we report a novel LCAT gene mutation in a patient which resulted in disruption of the disulfide bridges essential to the

* Corresponding author. Tel.: +81 42 7788111; fax: +81 42 7789371.
E-mail address: s-naito@med.kitasato-u.ac.jp (S. Naito).

0021-9150/$ – see front matter © 2013 Elsevier Ireland Ltd. All rights reserved.
http://dx.doi.org/10.1016/j.atherosclerosis.2013.02.034

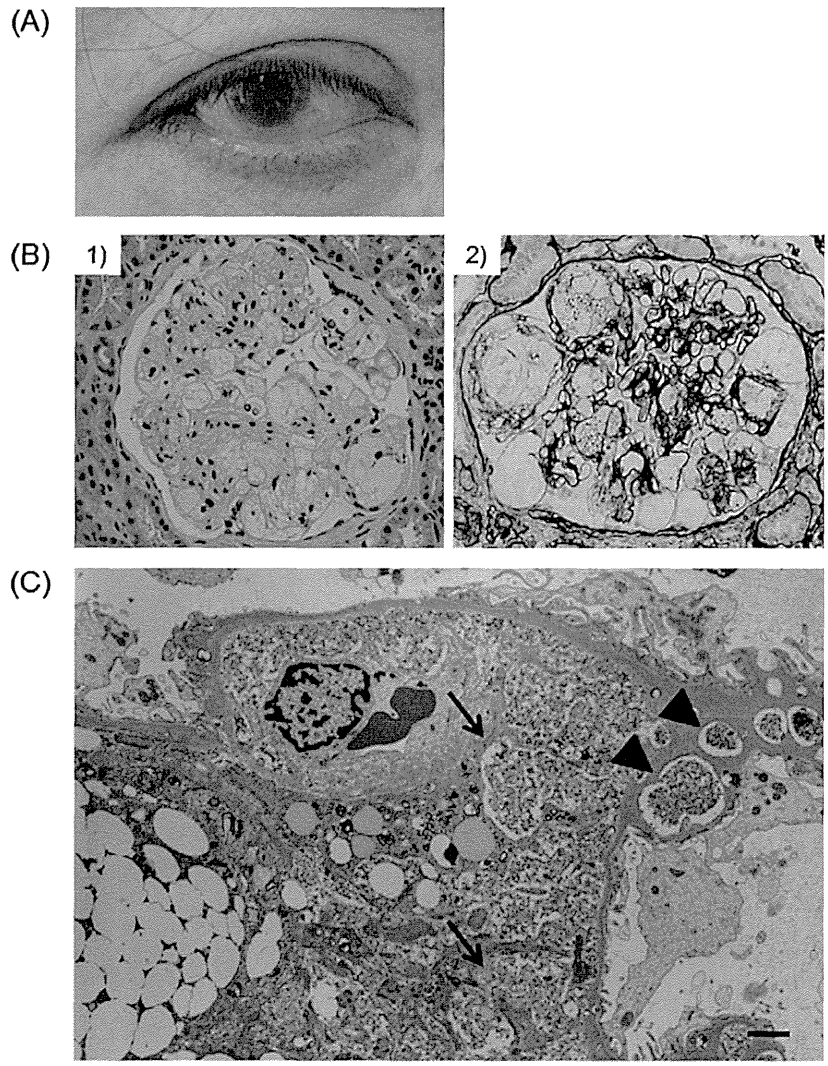

Fig. 1. Ocular and renal pathology (A) Corneal opacity in the patient. (B)-1) PAS staining of a renal biopsy specimen. 400×. An increase in cell number and matrix expansion are seen in the mesangial area of the glomerulus. Foam cell infiltration into capillary loops and the mesangial area are seen in the glomerulus. (B)-2) PAM staining shows irregular thickening and double contours in the glomerular basement membrane (GBM). Foam cells within granular structures are present in the capillary lumen. (C) Electron micrograph of the glomerulus shows the presence of clear vacuoles containing granular structures in the mesangium (↓) and within the GBM (▼). 3000×. Bar = 2 μm.

enzyme lid region. This patient had a complete deficiency in LCAT activity and renal insufficiency. We also investigated the effects of a fat-restriction diet and administration of an ARB on plasma lipoprotein profiles and proteinuria in this patient.

2. Materials and methods

2.1. Biochemical and genetic analysis

Biochemical and urine samples were analyzed by enzymatic methods using a chemical autoanalyzer (Hitachi Co., Tokyo, Japan). Esterified cholesterol concentrations were calculated as the difference between total and free cholesterol. LDL-cholesterol was determined a Determiner-L LDL-C (Kyowa Medex, Tokyo, Japan). LCAT activity in serum was measured using a colorimetric method for analyzing cholesterol esterification rate (CER) with synthetic dipalmitoyl lecithin sol [11]. Alpha-LCAT activity was also measured using Anasolb LCAT® (Sekisui Medical, Tokyo, Japan). Genomic DNA was purified from plasma with a QIAamp DNA kit (QIAGEN, Hilden, Germany). Genomic fragments were amplified by PCR, followed by agarose gel purification and direct sequencing. The entire sequence of the *lcat* gene locus thereby obtained was compared with a reference sequence (NM_000229) to identify nucleotide substitution. The study was approved by the Ethics Committee of Chiba University School of Medicine, and informed consent was obtained from the patient. Both parents were deceased, and informed consent for genetic analysis was not obtained from her younger sister, who shows corneal opacity.

2.2. Lipoprotein analysis

The serum lipoprotein profile was determined by polyacrylamide gel disc electrophoresis [12]. Two-dimensional electrophoresis was performed as described previously [13]. Lipoproteins were also evaluated by agarose gel electrophoresis using the rapid electrophoresis system [14–17]. After electrophoresis, cholesterol and triglycerides in the plates were separately stained and analyzed with a Cho/Trig COMBO kit according to the

manufacturer's instructions (Helena Laboratories, Saitama, Japan). Using the serum total cholesterol and TG concentrations in the blood samples, concentrations of cholesterol and TG in each fraction were determined using the detected ratio of cholesterol and TG after automatic densitometric analysis.

3. Results

3.1. Patient

A 61-year-old Japanese woman was transferred to the Department of Nephrology, Kitasato University Hospital. She complained of dyspnea on walking for the preceding five months, and eyelid and pretibial edema for one month. Family history showed her married parents were cousins, and that her younger sister had corneal opacity and mental retardation. She had anemia (Hemoglobin 9.5 g/dl) bilateral corneal opacities (Fig. 1A) and pitting edema. Urinalysis revealed proteinuria at 2 g/day, 1 + microscopic hematuria, and an N-acetyl-β-D-glucosaminidase (NAG) level of 29.1 unit/L (normal range: 1–4.2). Blood chemistry showed total protein 6.4 g/dL, albumin 3.4 g/dL, total cholesterol 235 mg/dL, TG 235 mg/dL, HDL-cholesterol 22 mg/dL, LDL-cholesterol 39 mg/dL, urea nitrogen 40 mg/dL, creatinine 1.83 mg/dL, and uric acid 8.2 mg/dL. CER of normal sera without heat inactivation was 96.3 ± 10.4 nmol/ml/h ($n = 3$), indicating normal LCAT activity. In contrast, CER of patient sera without heat-inactivation was 16.3 nmol/ml/h, which was below the CER of heat-inactivated normal sera (21.3 ± 1.8 nmol/ml/h, $n = 3$), indicating the total loss of LCAT activities in the patients. The 84 units of alpha-LCAT activity in patient serum measured by Anasorb LCAT® was also markedly low as compared with a standard level of 382–512 units. No abnormalities on chest X-ray, electrocardiography or echography findings were detected in either kidney. The renal biopsy specimen showed glomerular mesangial expansion, and foam cell infiltrates into glomerular tufts and mesangium. PAM staining revealed irregular thickening, double contouring, and vacuolation of the glomerular basement membrane (GBM) (Fig. 1B). Electron microscopic findings revealed numerous small vacuoles and granular structures within the vacuoles in the GBM and mesangial matrix (Fig. 1C). Immunofluorescence revealed negative staining for immunoglobulins of IgG, IgA and IgM, and for complement components of C1q, C4 and C3. These findings are consistent with the findings of LCAT deficiency.

3.2. Gene analysis

Direct sequencing of the *lcat* gene and comparison with a reference sequence (NM_000229) showed that the proband had a novel homozygous G to A nucleotide substitution in exon 2 resulting in Cys74Tyr [c.293 G > A (p.Cys74Tyr)]. The amino acid substitution was a novel mutation in the lid region of the LCAT protein. The substituted cysteine was one of four cysteine amino acid residues which formed the disulfide bonds in construction of the enzyme lid structure [23].

3.3. Lipid and lipoprotein profiles

Serum TG and free cholesterol values were higher than normal, while cholesterol ester, LDL-cholesterol and HDL-cholesterol values appeared lower (Table 1). Densitometric analysis for lipid staining of lipoproteins on disc polyacrylamide gel electrophoresis of serum showed a significant decrease in α and preβ-β positions, and a tiny abnormal "midband" localized on preβ-β position (Fig. 2A). Two-dimensional gel electrophoresis followed by immunodetection for apoprotein showed that distribution of apoprotein was shifted to the smaller HDL particles, indicating that the maturation of HDL particles was impaired (Fig. 2B). The production of LDL particles was thus severely disturbed, as evidenced by the presence of an abnormal "midband" lipoprotein and the disturbed maturation of HDL particles resulting in a severe decrease in HDL lipoprotein.

Table 1
Lipid profiles in a patient with LCAT deficiency following a fat-restriction diet and administration of losartan for 8 months. Lipid profiles at admission and after adoption of a fat-restriction diet consisting of 10 g fat, 45 g protein and 1570 kcal energy per day and administration of losartan 50 mg for 8 months on lipid profile in a patient with LCAT deficiency.

Lipid fraction		Normal value	At admission	At 8 months of treatment
Total cholesterol	(mg/dl)	120–220	235	80
Triglyceride	(mg/dl)	30–150	235	142
LDL-cholesterol	(mg/dL)	70–139	39	33
HDL-cholesterol	(mg/dL)	40–96	22	19
Free cholesterol	(mg/dL)	30–65	205	71
Cholesterol ester	(mg/dL)	90–200	30	9
Free/total cholesterol	(%)	70–80	87	88

Cholesterol and TG staining for lipoproteins which migrate to the α-position on agarose gel electrophoresis could not be seen in the serum at admission (Fig. 3A). Lipoproteins which migrate to the preβ-position were also decreased on both cholesterol and TG staining at admission (Fig. 3A), whereas lipoproteins which migrate to the β-position showed broad bands in both cholesterol and TG staining. The amount of cholesterol and TG in each lipoprotein fraction of serum at admission is shown in Table 2. Apolipoproteins AI and AII, which are predominantly contained in HDL-lipoprotein,

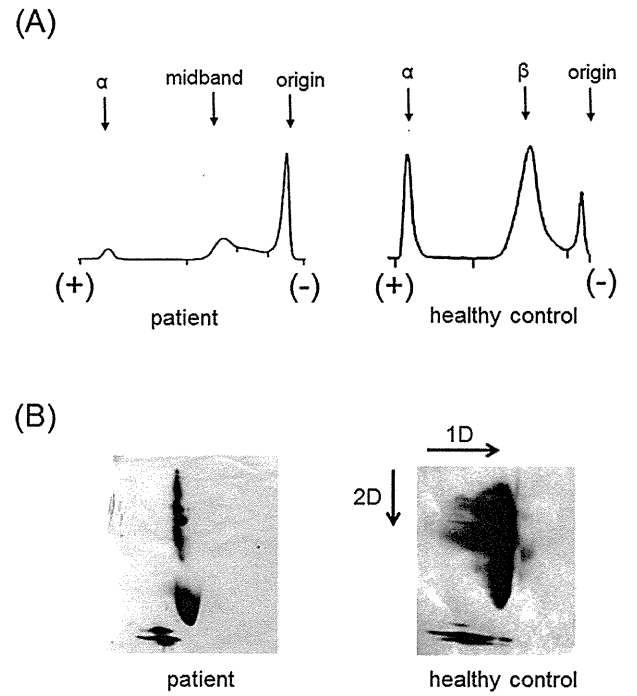

Fig. 2. Densitometric analysis of lipoproteins on disc polyacrylamide gel electrophoresis in the patient and a healthy control. (A) Serum at admission shows an increase in original position lipoproteins, a decrease in α-position lipoproteins, and the appearance of midband lipoproteins instead of β-position lipoproteins. (B) Two-dimensional disk electrophoresis consisting of charge separation for the first dimension and molecular weight separation for the second dimension followed by immunostaining for apolipoprotein. Apolipoprotein distribution was shifted towards the smaller HDL particles, indicating that the maturation of HDL particles in this patient was impaired.

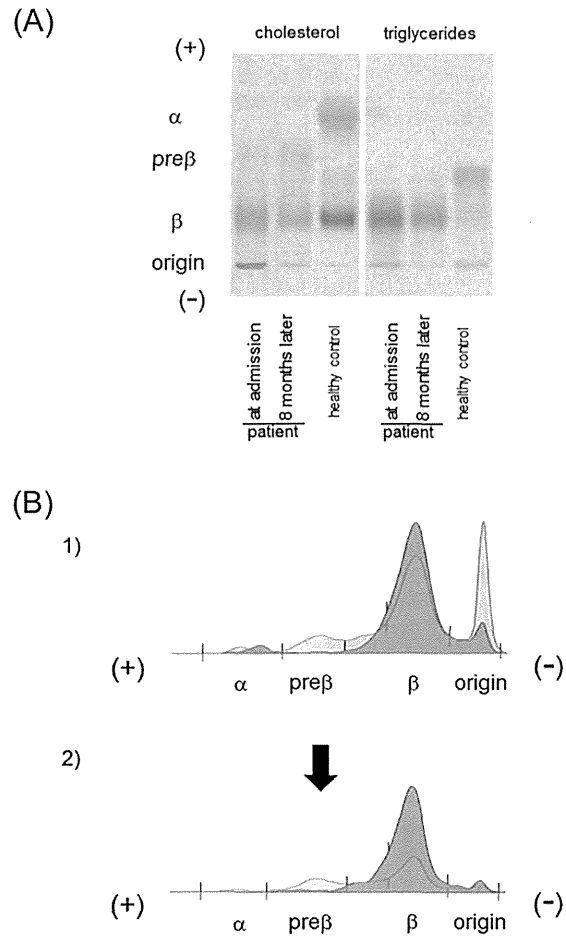

Fig. 3. Staining patterns for cholesterol and triglycerides in lipoproteins on agarose gel electrophoresis. (A) In cholesterol staining, the lipoproteins at original position increased, while the lipoproteins at α- and β-position decreased in the patient at admission compared with those of a healthy control. After 8 months on a fat-restriction diet and administration of losartan 50 mg, a decrease in original position lipoproteins is seen. In triglyceride staining, the serum sample at admission shows a decrease in preβ-position lipoproteins and increase in β-position lipoproteins compared with levels of a healthy control. (B) Densitometric analyzes for staining pattern. Cholesterol staining is shown as a red area, and triglycerides staining as a blue area. (B)-1) Staining patterns for lipoproteins in the patient's serum at admission. (B)-2) Staining patterns for lipoproteins in the patient's serum at 8 months after a fat-restriction diet and administration of losartan 50 mg. Original and β-position lipoproteins stained for cholesterol at admission have decreased after treatment for 8 months.

were decreased at admission (Table 2), whereas apolipoprotein CII and E were increased (Table 2).

3.4. Effects of a fat-restriction diet on LCAT deficiency-induced lipid profile and kidney disease

The patient was prescribed a fat-restricted diet consisting of meals containing 10 g of fat, 45 g of protein and 1570 kcal of energy during admission, and treatment with losartan, an ARB, was started by single daily administration at 50 mg from 14 days after admission. This treatment was continued following discharge, and follow-up at 8 months showed that compliance with both the diet and medication was good. Her body weight decreased from 64 to 52 kg at 6 month after the start of the fat-restricted diet, and was thereafter maintained. At one year of treatment, her proteinuria had decreased from 2.04 g/g·creatinine (Cr) to 0.62 g/g·Cr, and her serum Cr level had decreased from 1.83 mg/dl to 1.10 mg/dl.

Table 2
Apolipoprotein profile in a patient with LCAT deficiency before and after treatment with a fat-restriction diet and administration of losartan for 8 months. Apolipoprotein profile at admission, and effect of a fat-restriction diet consisting of 10 g fat, 45 g protein, and 1570 kcal energy per day for 8 months on apolipoproteins in a patient with LCAT deficiency.

Apolipoprotein fraction		Normal values	At admission	After 8 months of treatment
apoA-I	(mg/dL)	126–165	39	34
apoA-II	(mg/dL)	24–33.3	5.1	3.3
apoB	(mg/dL)	66–101	63	55
apoC-II	(mg/dL)	1.5–3.8	5.6	1.3
apoC-III	(mg/dL)	5.4–9.0	8.6	3.5
apoE	(mg/dL)	2.8–4.6	10.8	5.4

Changes in lipid and apolipoprotein fractions in sera samples collected at admission and 8 months of treatment are shown in Tables 1 and 2, respectively. Surprisingly, adoption of the fat-restriction diet resulted in a decrease in cholesterol, while TG contents and abnormal lipoproteins migrated to their original position (Table 2, Fig. 3A&B). The cholesterol content of lipoprotein at the β-position was also substantially decreased (Table 2, Fig. 3A&B). These data showed that the decrease in abnormal lipoproteins at the original position and change in lipid content in β-lipoproteins were the result of the fat-restriction diet and administration of an ARB.

4. Discussion

In this study, we report a patient with LCAT deficiency who experienced progressive renal dysfunction, proteinuria, anemia and corneal opacity. Her renal biopsy specimen showed many foam cell infiltrates into glomerular capillary tufts and mesangium, and numerous clear vacuoles containing granular structures within the GBM and mesangial matrix. Glomerular foam cells infiltrates are a characteristic feature of LCAT deficiency [18–20]. The numerous clear vacuoles within the GBM and mesangial matrix are also consistent with the findings of a previous study of LCAT deficiency [21]. However, the findings in our patient were not consistent with the structures of odd-shaped electron-dense materials with a membranous profile within clear vacuoles described in that study [21]. Differences in structure in clear vacuoles may be related to patient age or lipid composition in the vacuoles. It is conceivable that the glomerular lipid deposits are fully or partially composed of LpX, a cationized lipoprotein [22]. The glomerular charge barrier is composed of negatively-changed proteins and may be influenced by deposited cationized lipoproteins, resulting in the exacerbation of proteinuria. Indeed, agarose gel electrophoresis of serum from our patient at admission revealed a substantial amount of abnormal cationized lipoproteins suggestive of LpX at the original position (Fig. 3B-1). Proteinuria in this patient might have been induced by the deposition of this abnormal cationized lipoprotein into glomeruli.

Our patient had a novel mutation of Cys74Tyr in the lid region of LCAT protein. LCAT protein contains two functional disulfide bridges, Cys50-Cys74 and Cys313-Cys356 [23]. It appears likely that the Cys50-Cys74 bond was disrupted in our patient. In previous study, disruption of the Cys313-Cys356 bond by an amino acid substitution was shown to result in LCAT deficiency and early onset renal disease [10,24]. The former loop region in the LCAT protein, consisting of Tyr51-Asp73, has binding capacity for HDL- and LDL-cholesterol [25], and truncation of Lys53-Gly71 or Asp56-Leu68 from LCAT protein abolished the ability of LCAT protein to bind HDL- and LDL-cholesterol *in vitro* [26,27]. Our patient also showed a complete loss of LCAT activity, indicating that the former loop

region spanned by Cys50-Cys74 is essential for substrate recognition of LCAT in the esterification process [28]. Further *in vitro* and *in vivo* investigation of the effect of partial transformation of the Tyr51-Asp73 loop region on the cholesterol esterification process may contribute to our understanding of the biochemistry of enzyme–lipid interactions as well as the pathophysiology of LCAT deficiency.

Although sequential ultracentrifugation is a standard method in lipoprotein analysis, we applied agarose gel electrophoresis to detect abnormal LpX and LDL-like lipoproteins and for visualization of lipoproteins. Our patient had a significant increase in abnormal lipoproteins at the original position and a severe decrease in HDL-lipoprotein. Her serum also showed an abnormal midband lipoprotein and a disturbance in the maturation of HDL particles. We suggest that these lipoprotein abnormalities were due to the disturbance in esterification resulting from the loss of LCAT activity.

We also evaluated the effect of a fat-restriction diet and administration of an ARB on lipid profile, proteinuria and renal function in this patient. This treatment decreased proteinuria and resulted in a delay in the deterioration of renal function. A fat restriction diet obviously decreased her serum total-cholesterol and TG, except HDL-cholesterol and LDL-cholesterol at 8 months of treatment. The abnormal cationized lipoproteins at original positions, suggestive of LpX, disappeared after treatment. This disappearance of abnormal cationized lipoproteins in her serum after treatment may have induced a decreased in the amount of deposited cationized lipoproteins within the GBM, thereby resulting in restoration of the charge barrier in the GBM and decrease in proteinuria. The lipid content of lipoproteins at the β-position and the cholesterol content of the midband lipoprotein decreased also after treatment. Lipoproteins accumulating in the kidney are thought to be abnormal apoprotein E-rich lipoproteins which have migrated from the β-position [29], suggesting that the decrease in serum apoprotein E after treatment may be associated with the decrease in accumulated lipoproteins in the kidney. A fat-restriction diet in combination with ARB treatment may contribute to decrease in proteinuria and result in a delay in the deterioration of renal function in patients with LCAT deficiency.

Acknowledgments

We thank Yasuyuki Aoyagi and Sakiyo Asada for their genetic and biochemical analyzes. This study was supported in part by Health and Labour Sciences Research Grants for Translational Research for the research of primary hyperlipidemia, and by Nichibei Japan (H. B.).

References

[1] Glomset J. The mechanism of the plasma cholesterol esterification reaction: plasma fatty acid transferase. Biochim Biophys Acta 1962;65:128–35.
[2] Santamarina-Fojo S, Hoeg JM, Assman G, Brewer Jr HB. Lecithin cholesterol acyltransferase deficiency and fish eye disease. In: Scriver CR, Beaudet AL, Sly WS, et al., editors. In the metabolic and molecular bases of inherited disease. 8th ed. New York: McGraw-Hill Inc.; 2001. p. 2817–33.
[3] Norum KR, Gjone E. The effect of plasma transfusion on the plasma cholesterol esters in patients with familial plasma lecithin: cholesterol acyltransferase deficiency. Scand J Clin Lab Invest 1968;22:339–42.
[4] Murayama N, Asano Y, Kato K, et al. Effects of plasma infusion on plasma lipids, apoproteins and plasma enzyme activities in familial lecithin:cholesterol acyltransferase deficiency. Eur J Clin Invest 1984;14:122–9.
[5] Kuroda M, Aoyagi Y, Asada S, et al. Ceiling culture-derived proliferative adipocytes are a possible delivery vehicle for enzyme replacement therapy in lecithin:cholesterol acyltransferase deficiency. Open Gene Ther 2011;4:1–10.
[6] Kuroda M, Bujo H, Aso M, Saito Y. Adipocytes as a vehicle for ex vivo gene therapy: novel replacement therapy for diabetes and other metabolic diseases. J Diabetes Invest 2011;2:333–40.
[7] Yee MS, Pavitt DV, Richmond W, et al. Changes in lipoprotein profile and urinary albumin excretion in familial LCAT deficiency with lipid lowering therapy. Atherosclerosis 2009;205:528–32.
[8] Aranda P, Valdivielso P, Pisciotta L, et al. Therapeutic management of a new case of LCAT deficiency with a multifactorial long-term approach based on high doses of angiotensin II receptor blockers (ARBs). Clin Nephrol 2008;69: 213–8.
[9] Miarka P, Idzior-Waluś B, Kuźniewski M, Waluś-Miarka M, Klupa T, Sułowicz W. Corticosteroid treatment of kidney disease in a patient with familial lecithin-cholesterol acyltransferase deficiency. Clin Exp Nephrol 2011;15:424–9.
[10] Holleboom AG, Kuivenhoven JA, van Olden CC, et al. Proteinuria in early childhood due to familial LCAT deficiency caused by loss of a disulfide bond in lecithin:cholesterol acyl transferase. Atherosclerosis 2011;216:161–5.
[11] Nagasaki T, Akanuma Y. A new colorimetric method for determination of plasma lecithin-cholesterol acyltransferase activity. Clinica Chim Acta 1977;75:371–5.
[12] Narayan KA, Narayan S, Kummerou FA. Disk electrophoresis of human serum lipoproteins. Nature 1965;205:246–8.
[13] Asada S, Kuroda M, Aoyagi Y, et al. Disturbed apolipoprotein A-I-containing lipoproteins in fish-eye disease are improved by the lecithin:cholesterol acyltransferase produced by gene-transduced adipocytes in vitro. Mol Genet Metab 2011;102:229–31.
[14] Winkler K, Nauck M, Siekmeier R, März W, Wieland H. Determination of triglycerides in lipoproteins separated by agarose gel electrophoresis. J Lipid Res 1995;36:1839–47.
[15] Contois JH, Gillmor RG, Moore RE, Contois LR, Macer JL, Wu AH. Quantitative determination of cholesterol in lipoprotein fractions by electrophoresis. Clin Chim Acta 1999;282:1–14.
[16] Kido T, Kurata H, Matsumoto A, et al. Lipoprotein analysis using agarose gel electrophoresis and differential staining of lipids. J Atheroscler Thromb 2001;8:7–13.
[17] Zhang B, Matsunaga A, Saku K, Nakano S, Yamada T. Associations among plasma lipoprotein subfractions as characterized by analytical capillary isotachophoresis, apolipoprotein E phenotype, Alzheimer disease, and mild cognitive impairment. Arterioscler Thromb Vasc Biol 2004;24:e144–146.
[18] Chevet D, Ramee MP, Le Pogamp P, et al. Hereditary lecithin:cholesterol acyltransferase deficiency. Report of a new family with two afflicted sisters. Nephron 1978;212:212–9.
[19] Gjone E. Familial LCAT deficiency. Acta Med Scand 1973;194:353–6.
[20] Hovig T, Gjone E. Familial plasma lecithin: cholesterol acyltransferase (LCAT) deficiency. Ultrastructural aspects of a new syndrome with particular reference to lesions in the kidneys and the spleen. Acta Pathol Microbiol Scand A 1973;81:681–97.
[21] Magil A, Chase W, Frohlich J. Unusual renal biopsy findings in a patient with familial lecithin:cholesterol acyltransferase deficiency. Hum Pathol 1982;13: 283–5.
[22] Hovig T, Blomhoff JP, Holme R, et al. Plasma lipoprotein alterations and morphologic changes with lipid deposition in the kidneys of patients with hepatorenal syndrome. Lab Invest 1978;38:540–9.
[23] Yang CY, Manoogian D, Pao Q, et al. Lecithin:cholesterol acyltransferase. Functional regions and a structural model of the enzyme. J Biol Chem 1987;262:3086–91.
[24] Holleboom AG, Kuivenhoven JA, Peelman F, et al. High prevalence of mutations in LCAT in patients with low HDL cholesterol levels in the Netherlands: identification and characterization of eight novel mutations. Hum Mutat 2011;32:1290–8.
[25] Jonas A. Lecithin cholesterol acyltransferase. Biochim Biophys Acta 2000;1529:245–56.
[26] Jin L, Shieh JJ, Grabbe E, Adimoolam S, Durbin D, Jonas A. Surface plasmon resonance biosensor studies of human wild-type and mutant lecithin cholesterol acyltransferase interactions with lipoproteins. Biochemistry 1999;38:15659–65.
[27] Peelman F, Vanloo B, Perez-Mendez O, et al. Characterization of functional residues in the interfacial recognition domain of lecithin cholesterol acyltransferase (LCAT). Protein Eng 1999;12:71–8.
[28] Adimoolam S, Jonas A. Identification of a domain of lecithin-cholesterol acyltransferase that is involved in interfacial recognition. Biochem Biophys Res Commun 1997;232:783–7.
[29] Gröne EF, Walli AK, Gröne HJ, Miller B, Seidel D. The role of lipids in nephrosclerosis and glomerulosclerosis. Atherosclerosis 1994;107:1–13.

Arteriosclerosis, Thrombosis, and Vascular Biology

JOURNAL OF THE AMERICAN HEART ASSOCIATION

American Heart Association®

Lipoprotein Subfractions Highly Associated With Renal Damage in Familial Lecithin:Cholesterol Acyltransferase Deficiency

Masayuki Kuroda, Adriaan G. Holleboom, Erik S.G. Stroes, Sakiyo Asada, Yasuyuki Aoyagi, Kouju Kamata, Shizuya Yamashita, Shun Ishibashi, Yasushi Saito and Hideaki Bujo

Arterioscler Thromb Vasc Biol. 2014;34:1756-1762; originally published online May 29, 2014;
doi: 10.1161/ATVBAHA.114.303420
Arteriosclerosis, Thrombosis, and Vascular Biology is published by the American Heart Association, 7272 Greenville Avenue, Dallas, TX 75231

Print ISSN: 1079-5642. Online ISSN: 1524-4636

Lipoprotein Subfractions Highly Associated With Renal Damage in Familial Lecithin:Cholesterol Acyltransferase Deficiency

Masayuki Kuroda, Adriaan G. Holleboom, Erik S.G. Stroes, Sakiyo Asada, Yasuyuki Aoyagi, Kouju Kamata, Shizuya Yamashita, Shun Ishibashi, Yasushi Saito, Hideaki Bujo

Objective—In familial lecithin:cholesterol acyltransferase (LCAT) deficiency (FLD), deposition of abnormal lipoproteins in the renal stroma ultimately leads to renal failure. However, fish-eye disease (FED) does not lead to renal damage although the causative mutations for both FLD and FED lie within the same *LCAT* gene. This study was performed to identify the lipoproteins important for the development of renal failure in genetically diagnosed FLD in comparison with FED, using high-performance liquid chromatography with a gel filtration column.

Approach and Results—Lipoprotein profiles of 9 patients with LCAT deficiency were examined. Four lipoprotein fractions specific to both FLD and FED were identified: (1) large lipoproteins (>80 nm), (2) lipoproteins corresponding to large low-density lipoprotein (LDL), (3) lipoproteins corresponding to small LDL to large high-density lipoprotein, and (4) to small high-density lipoprotein. Contents of cholesteryl ester and triglyceride of the large LDL in FLD (below detection limit and 45.8±3.8%) and FED (20.7±6.4% and 28.0±6.5%) were significantly different, respectively. On in vitro incubation with recombinant LCAT, content of cholesteryl ester in the large LDL in FLD, but not in FED, was significantly increased (to 4.2±1.4%), whereas dysfunctional high-density lipoprotein was diminished in both FLD and FED.

Conclusions—Our novel analytic approach using high-performance liquid chromatography with a gel filtration column identified large LDL and high-density lipoprotein with a composition specific to FLD, but not to FED. The abnormal lipoproteins were sensitive to treatment with recombinant LCAT and thus may play a causal role in the renal pathology of FLD. (***Arterioscler Thromb Vasc Biol.* 2014;34:1756-1762.)**

Key Words: chromatography, gel ■ LDL ■ lecithin acyltransferase deficiency ■ renal insufficiency

Lecithin:cholesterol acyltransferase (LCAT)–deficiency syndromes are rare autosomal recessive diseases, characterized by hypo-α-lipoproteinemia and corneal opacity.[1,2] They are caused by mutations in the *LCAT* gene, of which 88 have been reported to date.[3] Severe mutations lead to familial LCAT deficiency (FLD), mild mutations lead to fish-eye disease (FED). In FLD, the mutant LCAT enzyme is either absent in plasma (not secreted from the hepatocyte or rapidly degraded on secretion) or exhibits no catalytic activity on any lipoprotein; in FED, LCAT cannot esterify cholesterol on high-density lipoprotein (HDL; loss of α-activity) but retains its activity on lipoproteins containing apolipoprotein B (β-activity).[1,2] Likely, the molecular difference is causal to the major clinical difference between FLD and FED: patients with FLD develop renal failure, whereas patients with FED do not.[2,4]

To prevent renal failure in patients with FLD, replacement therapy with recombinant enzyme is currently being developed.[5–8] Alternatively, we are developing a long-lasting gene therapy by transplantation of human *LCAT* gene-transduced autologous adipocytes.[7,9] Recombinant LCAT (rLCAT) secreted by the *LCAT* gene-transduced adipocytes corrected abnormal HDL subpopulations in sera of FED patients in vitro.[10]

LCAT catalyzes the esterification of cholesterol with acyl groups hydrolyzed from phospholipids, predominantly on HDL particles. This leads to mature lipoproteins with cores filled with cholesterol ester. LCAT dysfunction leads to decreased maturation of the HDL particle and to increased levels of both its substrates: unesterified cholesterol and phosphatidylcholine. In the absence of LCAT activity, abnormal lipid particles have been observed throughout lipoprotein fractions.[11–14] The HDL fraction contains disk-shaped particles in rouleaux and small spherical particles. Density-gradient ultracentrifugation followed by electron microscopy

Received on: August 9, 2013; final version accepted on: May 14, 2014.

From the Department of Genome Research and Clinical Application, Graduate School of Medicine (M.K., S.A., Y.A., H.B.) and Center for Advanced Medicine, Chiba University Hospital (M.K.), Chiba University, Chiba, Japan; Department of Vascular Medicine, Academic Medical Center, University of Amsterdam, Amsterdam, The Netherlands (A.G.H., E.S.G.S.); Department of Nephrology in Internal Medicine, Kitasato University Hospital, Sagamihara, Japan (K.K.); Department of Internal Medicine and Molecular Science, Osaka University Graduate School of Medicine, Suita, Japan (S.Y.); Division of Endocrinology and Metabolism, Department of Medicine, Diabetes Center, Jichi Medical University, Shimotsuke, Japan (S.I.); Chiba University, Chiba, Japan (Y.S.); and Department of Clinical-Laboratory and Experimental-Research Medicine, Toho University Sakura Medical Center, Sakura, Japan (H.B.).

The online-only Data Supplement is available with this article at http://atvb.ahajournals.org/lookup/suppl/doi:10.1161/ATVBAHA.114.303420/-/DC1.

Correspondence to Hideaki Bujo, MD, PhD, Department of Clinical-Laboratory and Experimental-Research Medicine, Toho University Sakura Medical Center, 564-1 Shimoshizu, Sakura, 285-8741, Japan. E-mail hideaki.bujo@med.toho-u.ac.jp

Arterioscler Thromb Vasc Biol **is available at http://atvb.ahajournals.org** **DOI: 10.1161/ATVBAHA.114.303420**

Nonstandard Abbreviations and Acronyms	
CE	cholesteryl ester
FC	free cholesterol
FED	fish-eye disease
FLD	familial lecithin:cholesterol acyltransferase deficiency
GFC	gel filtration column
HDL	high-density lipoprotein
HPLC	high-performance liquid chromatography
LCAT	lecithin:cholesterol acyltransferase
LDL	low-density lipoprotein
Lp	lipoprotein
LpX	lipoprotein-X
rLCAT	recombinant LCAT

revealed that the low-density lipoprotein (LDL) fraction contains 3 abnormal particles with different sizes, lipid composition, and associated apolipoproteins,[11,12] which were proposed to be important in the pathogenesis of renal manifestation in patients with FLD.[15–18] Of these, lipoprotein-X (LpX)[19,20] have been postulated to accumulate in glomeruli, potentially causing the renal damage observed in patients with FLD.[16–18] In 1 patient with FLD, lipid-lowering therapy led to a reduction of LpX and a concomitant reduction in proteinuria.[21] LpX is phospholipid (PL)-rich and free cholesterol (FC)–rich but triglyceride (TG)-poor particle without apolipoproteins, ranging in size between very low density lipoprotein and large LDL.[22]

To characterize the abnormal lipoproteins associated with the renal pathology of FLD, we characterized lipoprotein fractions by analyzing patients with different mutations and manifestations in comparison with another LCAT-deficiency syndrome, FED. We applied high-performance liquid chromatography with a gel filtration column (HPLC-GFC) for the first time to characterize the above abnormal lipoproteins and in fact identified lipoprotein subfractions specific to FLD. The lipid contents and particle size were biochemically determined, and the responsiveness of the lipoproteins against incubation with rLCAT was investigated in vitro.

Materials and Methods

Materials and Methods are available in the online-only Supplement.

Results

Lipoprotein Subfractions Specific to LCAT-Deficiency Syndromes

Five patients with FLD (1–5) and 4 patients with FED (6–9) were compared with 4 nonaffected normolipidemic controls. Clinical and molecular characteristics and lipid profiles of the patients are given in Tables 1 and 2, respectively. Ultracentrifugation fractionation followed by determination of lipid contents was performed in patients 1, 2, and 5 (Table I in the online-only Data Supplement). LCAT α-activities in the patients' sera were all <2% of reference. As expected in LCAT deficiency, mature HDL particles found at fraction (Fr.) 16 and 17 of unaffected controls were absent in the 9 patients (Figure 1). Although the lipid profiles of patients were heterogeneous, HPLC-GFC showed 4 lipoprotein fractions in sera of patients with FLD and FED that were not present in sera of unaffected controls: large lipoproteins (>80 nm) in Fr. 1 (Lp1), lipoproteins corresponding to large LDL in Fr. 8 (or Fr. 7–10; Lp8), lipoproteins corresponding to very small LDL and large HDL in Fr. 12 to 16 (Lp12–16), and lipoproteins corresponding to small HDL in Fr. 18 to 20 (Lp18–20). The levels of cholesterol, TG, and PL in these specific fractions varied among the 9 patients (Figure 1). Serum apolipoprotein analyses of Fr. 7 to 10, Fr. 13 to 15, and Fr. 18 to 20 in 3 patients (1, 2, and 5) showed that Fr. 13 to 15 and Fr. 18 to 20 were rich in apolipoprotein A as normolipidemic control although varied among patients (Figure I in the online-only Data Supplement). Apolipoprotein Cs were also rich in Fr. 18 to 20 but not in Fr. 13 to 15. Apolipoprotein B was mostly distributed in Fr. 8 to 10 among the 3 fraction categories. Apolipoprotein E was abundant in all 3 fraction categories when compared with that in the control.

Abnormal Lipoproteins Are Present in FLD Regardless of Degree of Proteinuria

To study the relationship between lipoproteins and the degree of proteinuria in patients with FLD, lipoproteins between 2 sibling patients with FLD homozygous for the C337Y mutation in LCAT were compared (Figure 1, patients 1 and 3). Patient 1 had proteinuria in the nephrotic range (6 g/24 h), whereas patient 3 had only mild proteinuria (0.45 g/L).[23] All 4 abnormal lipoproteins were present in both patients (Figure 2A), although 3 lipoproteins (Lp1, Lp8, and Lp18-20) were lower in the younger patient.

Table 1. Clinical and Molecular Characteristics of Patients With Lecithin:Cholesterol Acyltransferase Deficiency

Patient	Sex	Age, Y	Race	Renal Failure/Proteinuria	Corneal Opacity	Anemia	CAD	Phenotype	AA Substitution	References
1	F	17	White (Morocco)	6 g/24 h	+	11.4 g/dL	–	FLD	C337Y	23
2	F	61	Japanese	2 g/24 h	+	9.5 g/dL	–	FLD	C98Y	24
3	F	12	White (Morocco)	0.45 g/L	+	9.2 g/dL	–	FLD	C337Y	23
4	F	63	Japanese	0.23 g/24 h	+	10.3 g/dL	–	FLD	G203R	25
5	M	68	Japanese	0.5 g/L	+	6.6 g/dL	–	FLD	G54S	26
6	M	38	Japanese	–	+	–	–	FED	T147I	10
7	M	58	White (Dutch)	–	+	–	–	FED	T147I	None
8	M	36	White (Dutch)	–	+	–	–	FED	W99S/T147I	27
9	F	30	White (Dutch)	–	+	–	–	FED	T147I/V333M	28

Patients 8 and 9 are compound heterozygotes; others are homozygotes for the indicated mutations. AA indicates amino acid; CAD, coronary artery disease; F, female; FED, fish-eye disease; FLD, familial lecithin:cholesterol acyltransferase deficiency; and M, male.

Table 2. Lipid Profiles of Patients With Lecithin:Cholesterol Acyltransferase Deficiency

Patients	TC	TG	HDL-C	LDL-C	CE/TC
1	109	179	5.8	67	0
2	123	307	9.3	52	0.13
3	47	56	10.1	26	0
4	47	89	6.3	23	0.13
5	56	59	2.0	42	0
6	85	120	4.0	57	0.57
7	133	120	4.7	104	0.54
8	144	205	3.9	99	0.57
9	98	118	4.9	70	0.39

Values for LDL-C were calculated according to Friedewald et al.[29] CE/TC indicates cholesteryl ester/total cholesterol ratio; HDL-C, high-density lipoprotein-cholesterol; LDL-C, low-density lipoprotein-cholesterol; TC, total cholesterol; and TG, triglyceride.

Next, lipoprotein profiles of a patient with FLD with homozygous for the C98Y[24] mutation before and after a fat-restricted diet, which led to a reduction of proteinuria from 2.0 g/gCr to 0.6 g/gCr, were compared (Figure 1, patient 2). All 4 lipoproteins remained present after the diet although Lp1 and Lp8 were decreased to some extent (Figure 2B).

Lp8 and Lp12 to 16 Are Specific to FLD and Not to FED

Next, composition of the 4 Lps was analyzed (Figure II in the online-only Data Supplement). In all lipoproteins, cholesteryl ester (CE) was absent in FLD and low in Lp1, Lp12 to 16, and Lp18 to 20 in FED (panel A). PL in Lp8 was significantly lower in FLD when compared with that in FED (panel D). PL and FC were increased in Lp12 to 16 in FLD when compared with that in FED (panels B and D). FC, TG, and PL in both Lp1 and Lp18 to 20 did not differ between FLD and FED.

Lp8 Is a Large LDL, Rich in FC, PL, and TG, and Different From LpX

In comparison with unaffected controls and to patients with FED, CE in the LDL fractions of FLD sera was significantly decreased, whereas TG was increased (Figure 3A). In patients with both FLD and FED, FC, TG, and PL in Fr. 8 were significantly higher than in Fr. 9, whereas in controls, FC, TG, and PL in Fr. 8 were significantly lower than in Fr. 9 (Figure 3B). As a result, average sizes of Lp8 (Fr. 7–10) in FLD were significantly increased when compared with normal, whereas averaged particle size in FLD was lower than those in FED because of the severe deficiency of CE (Figure 3C). The composition of Lp8 in our patients with FLD is consistent with the previously reported FLD-LDL, and not consistent with the lipid characteristics of LpX.

Abnormal Lipid Compositions of FLD-Specific Lps Are Ameliorated by In Vitro Incubation With rLCAT

In vitro rLCAT incubation was performed followed by HPLC-GFC analyses (Figure III in the online-only Data Supplement). Incubation of patients' sera with rLCAT increased CE, TG, and PL in Fr. 16 to 18 in both FLD and FED (Figure IV in

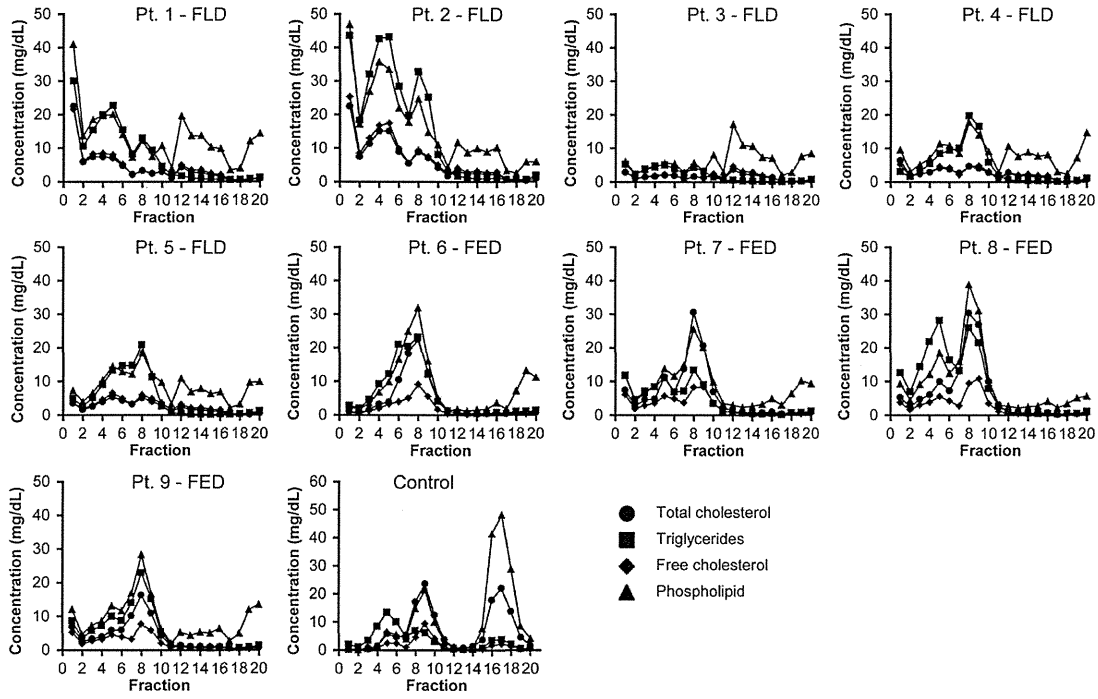

Figure 1. Lipoprotein profiles in patients with familial lecithin:cholesterol acyltransferase deficiency (FLD) by high performance liquid chromatography (HPLC) with gel filtration column (GFC). Sera from patients with 5 FLD (patients [Pts.] 1–5) and 4 Fish-eye disease (FED; Pts. 6–9) were subjected to lipoprotein size fractionation with concomitant determination of lipid concentrations in each fraction by high-performance liquid chromatography-GFC analyses. Representative result is shown for normolipidemic subjects. Concentrations of total cholesterol (●), triglyceride (■), free cholesterol (♦), and phospholipid (▲; *y* axis) in each fraction (*x* axis) are shown.

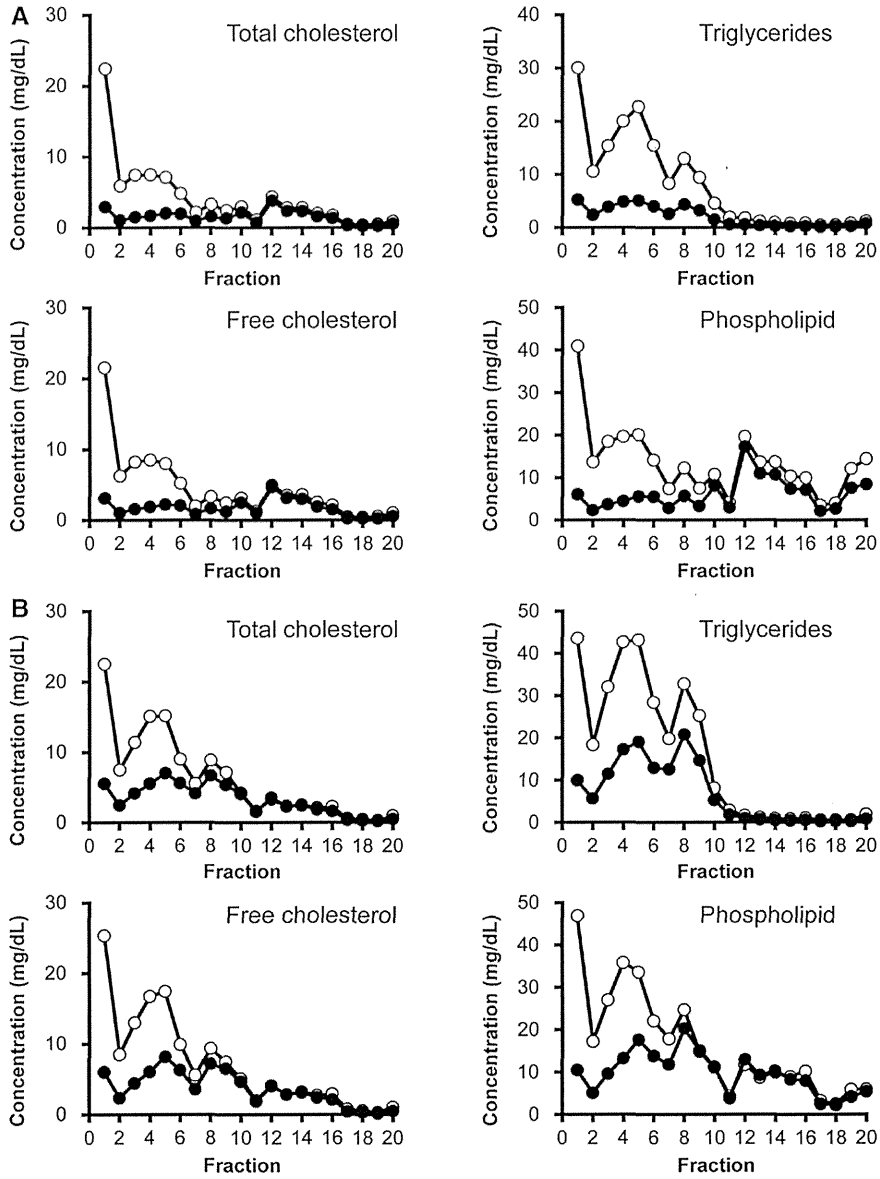

Figure 2. Differences in lipoproteins in patients with familial lecithin:cholesterol acyltransferase deficiency (FLD) with or without renal insufficiency. **A**, Lipoprotein profiles were compared between a patient with FLD with nephrotic range proteinuria (patient 1, o) and patient 3 with mild proteinuria (●). **B**, Lipoprotein profiles were compared between before (o) and after (●) fat-restricted diet.

the online-only Data Supplement), indicating LCAT-mediated maturation of HDL. CE and PL contents of Lp8 were significantly increased and decreased, respectively, in FLD after incubation with rLCAT, whereas TG content was not significantly altered (Figure 4A and 4B). In FED, composition of Lp8 was not significantly altered by the treatment (Figure 4A and 4B). On incubation with rLCAT, Lp8 increased in size in FLD and it decreased in size in FED (Figure 4C). However, FC and PL in Lp12 to 16 decreased on incubation (Figure 4D).

Discussion

In this study, 4 lipoprotein fractions specific to LCAT-deficiency syndromes were identified by the HPLC-GFC analysis of samples from genetically diagnosed patients with different mutations and manifestations. Two of these had lipid compositions that were specific to FLD and thus may be involved in causing the renal damage that characterizes FLD. In vitro incubation with rLCAT corrected the abnormal fractions.

Lp1, one of the abnormal lipoproteins characteristic to LCAT-deficiency syndrome, was rich in TG and PL, and associated with the degree of proteinuria in 2 siblings with FLD, and was decreased on fat restriction in another patient with FLD (Figure 2). Indeed, abnormal lipoproteins with size of ≈100 nm corresponding to Lp1 have been identified in patients with LCAT deficiency with renal failure.[2,11,12,15] The lipid composition of Lp1 did not change on incubation with rLCAT (data not shown). Together, this suggests that Lp1 is most likely secondary to renal failure rather than directly caused by LCAT deficiency.

As opposed to controls, Fr. 8 was richer in total cholesterol, TG, FC, and PL than Fr. 9 in the patients with LCAT